A Soluble Molecular Variant of the Semiconducting Silicondiselenide

Kartik Chandra Mondal, Sudipta Roy, Birger Dittrich,* Bholanath Maity, Sayan Dutta, Debasis Koley,* Suresh Kumar Vasa, Rasmus Linser, Sebastian Dechert, and Herbert W. Roesky,*

Supporting Information

Content:

(S1) Synthesis

All reactions and handling of reagents were performed under an atmosphere of dry nitrogen or argon using standard Schlenk techniques or a glove box where the O_2 and H_2O levels were usually kept below 1 ppm. Me_2-cAAC, Cy-cAAC, (Me_2-cAAC)→$SiCl_4$ (**1a**) and (Cy-cAAC)→$SiCl_4$ (**1b**) were prepared according to literature methods.[S1-S3] Solvents were purified with the M-Braun solvent drying system. Solution NMR spectra were recorded on Bruker Avance 200, Bruker Avance 300, and Bruker Avance 500 MHz NMR spectrometers. Deuterated NMR solvent THF-d_8 and C_6D_6 were dried by stirring for 2 days over Na/K alloy followed by distillation in vacuum. EI-MS spectra were obtained with a Finnigan MAT 8230 or a Varian MAT CH5 instrument (70 eV) by EI-MS methods. Elemental analyses were performed by the Analytisches Labor des Instituts für Anorganische Chemie der Universität Göttingen. Melting points were measured in sealed glass tubes on a Büchi B-540 melting point apparatus.

$(Me_2\text{-cAAC})_2Si_2$ (**2a**): The mixture of $(Me_2\text{-cAAC})\rightarrow SiCl_4$ (**1**) (779 mg; 1.71 mmol) and KC_8 (924 mg; 6.84 mmol) was taken into a 100 mL round bottom flask and 40 mL of THF was added at -78 °C. The mixture was stirred for 1.5 h and filtered through celite to get a dark red violet filtrate which was dried under vacuum and extracted with *n*-hexane (60 mL). The evaporation of solvent under vacuum gave dark black needles from the violet solution in 52% yield. The X-ray single crystal analysis revealed the molecular structure of **2a**. Elemental analysis found in % (calcd) for $C_{40}H_{62}N_2Si_2$: C, 76.30 (76.61); H, 9.89 (9.96); N, 4.38 (4.46). Melting point 180-181 °C, decomposition point 200-205 °C, Uv-visible bands at 516.7, 397.0 , and 377.8 nm. The needles of **2a** are sensitive to air and moisture. They loose their colors from dark purple to colorless powder of Me_2-cAAC=O[S5] within ten min when exposed to air.

^{1}H NMR (500 MHz, 298 K, C_6D_6, ppm) δ: 7.12 (d, J = 3.3 Hz, 1H), 7.10 (d, J = 8.2 Hz, 4H), 7.08 (d, J = 2.6 Hz, 1H), 3.12 (dq, J = 13.3, 6.6 Hz, 4H), 1.77 (s, 4H), 1.71 (s, 12H), 1.69 (d, J = 6.6 Hz, 12H), 1.21 (d, J = 6.7 Hz, 12H), 1.06 (s, 12H).

^{13}C NMR (126 MHz, 298 K, C_6D_6, ppm) δ: 236.69 ($C_{carbene}$), 148.55, 135.24, 129.34, 125.67, 71.59, 54.74, 50.29, 32.18, 29.85, 29.45, 28.82, 25.17.

^{29}Si NMR (99 MHz, 298 K, C_6D_6, ppm) δ: 252.34.

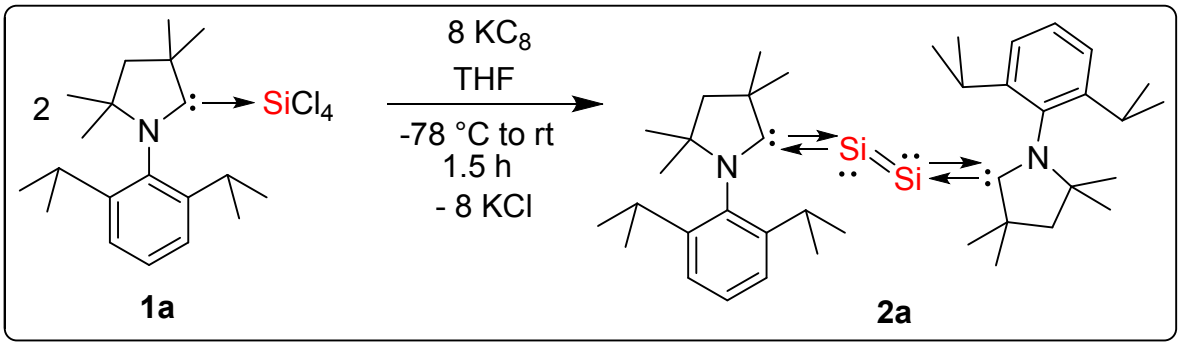

Scheme S1: Synthesis of compound **2a** from **1a** (cAAC = Me_2-cAAC).

Compound **2b**: The mixture of (Cy-cAAC)$\rightarrow SiCl_4$ (**1b**) (1680 mg; 3.40 mmol) and KC_8 (924 mg; 13.68 mmol) was taken into a 100 mL round bottom flask and 50 mL of THF were added at -78 °C. The mixture was stirred for 1.5 h and filtered through celite to get a dark red violet filtrate which was dried under vacuum and extracted with *n*-hexane (2×70 mL). The evaporation of solvent under vacuum gave dark black needle like crystals of **2b** from the purple solution in 54% yield. Elemental analysis found in % (calcd) for $C_{46}H_{70}N_2Si_2$: C, 78.18 (78.12); H, 9.86 (9.97); N, 3.95 (3.96). Melting point 188-190 °C, Uv-vis bands at 528 and 416 nm.

^{1}H NMR (500 MHz, 298 K, C_6D_6, ppm) δ: 7.13 (t, J = 4.9 Hz, 3H), 7.11–7.09 (m, 3H), 3.16–3.06 (m, 4H), 2.97 (dd, J = 18.0, 7.5 Hz, 4H), 1.84 (s, 4H), 1.69 (d, J = 6.6 Hz, 12H), 1.63–1.56 (m, 10H), 1.28 (dd, J = 15.2, 7.8 Hz, 6H), 1.23 (d, J = 6.7 Hz, 12H), 1.09 (s, 12H).

^{13}C NMR (126 MHz, 298 K, C_6D_6, ppm) δ: 234.77 ($C_{carbene}$), 148.04, 134.99, 128.79, 125.27, 71.53, 55.30, 48.63, 38.66, 29.81, 29.05, 28.26, 25.84, 24.92, 23.83.

^{29}Si NMR (99 MHz, 298 K, C_6D_6, ppm) δ: 249.13.

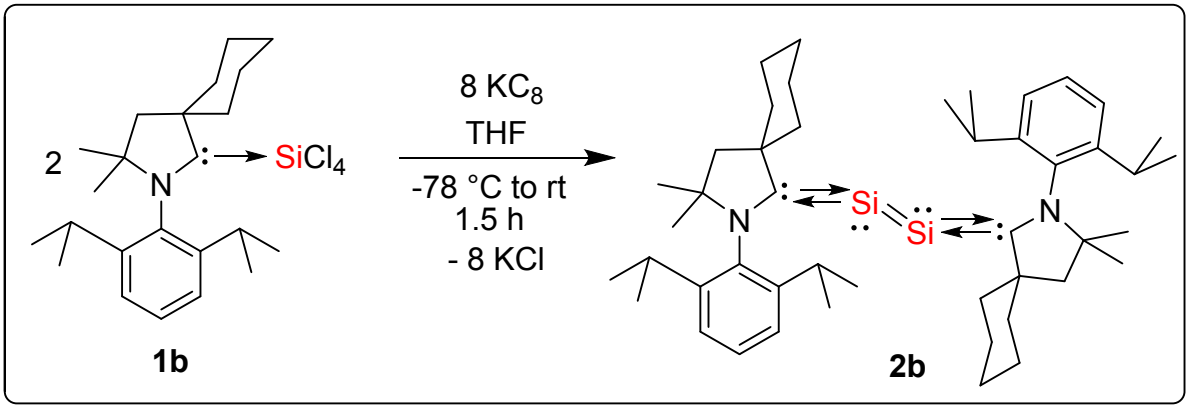

Scheme S2: Synthesis of compound **2b** from **1b** (cAAC = Cy-cAAC).

Compound **3a**: Compound **2a** (0.2 mmol; 126 mg) is dissolved in THF (25 mL) to obtain a dark purple solution which is cooled to -78 °C and passed into another flask containing black selenium powder (0.8 mmol; 64 mg) (**2a**:Se = 1:4 molar ratio). The temperature of the solution is raised to room temperature over 30 min. The mixture is stirred for 3 h to obtain a brown solution with unreacted selenium powder. Stirring was continued for another 2.5 h to produce a clear orange solution. The volume of THF solution is reduced to 2 mL under vacuum. Finally, 3 mL of toluene are added and the orange solution is stored at -32 °C in a freezer to form small orange blocks of **3a** in 30% yield. Elemental Analysis for $C_{40}H_{62}N_2Se_4Si_2$ (cald.): C, 50.86 (50.95); H, 6.71 (6.63); N, 2.93 (2.97). UV-vis absorption band at 422 nm (recorded on solid sample). The infrared (IR) spectrum of **3a** (measured in the range of 400-4000 cm^{-1}) showed a sharp absorption at 547 cm^{-1}. Additionally, **3a** is studied by Raman spectroscopy (see SI). Orange powders of **3a** decompose above 285 °C to give light yellow solids of Me_2-cAAC=Se.[S4] **3a** is partially soluble in both *n*-hexane and THF. EI-MS mass spectrum of **3a**: (*m/z*(100%); 944.2).

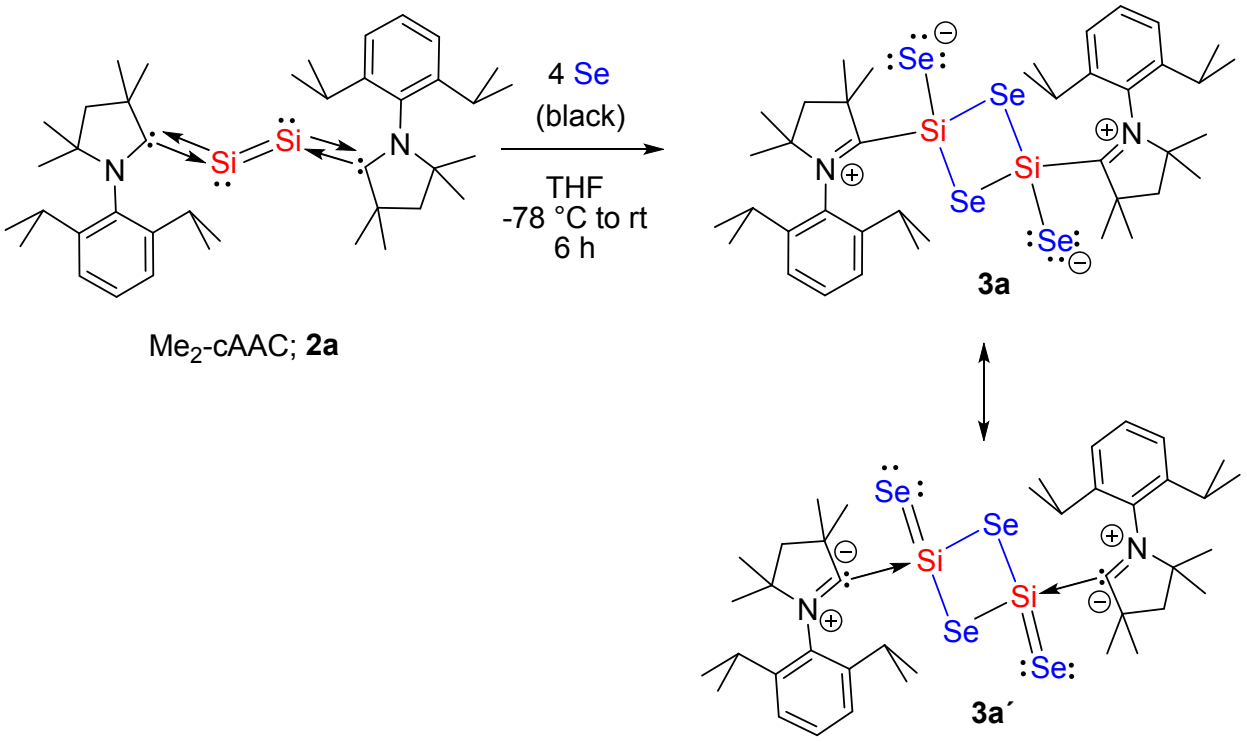

Scheme S3: Synthesis of compound **3a** from **2a**.

Compound **3b**: Compound **2b** (0.2 mmol; 141 mg) is dissolved in THF (25 mL) to obtain a dark purple solution which is cooled to -78 °C and passed into another flask containing black selenium powder (0.8 mmol; 64 mg) (**2b**:Se = 1:4 molar ratio). The temperature of the solution is raised to room temperature (rt) over 30 min. The mixture is stirred for 1.5 h at rt to obtain a brown solution with unreacted selenium powder. The reaction of **2b** is faster than that of **2a**. Stirring was continued for another 2 h to produce a clear orange solution. The volume of THF solution is reduced to 2 mL under vacuum. Concentrated orange colored THF solution is stored at -32 °C in a freezer to form small orange rods of **3b** in 32% yield. Compound **3b**: Elemental Analysis for $C_{46}H_{70}N_2Se_4Si_2$ (cald.): C, 53.8 (54.0); H, 6.86, (6.90); N, 2.71 (2.74). **3b** is partially soluble in *n*-hexane but completely soluble in THF. Orange powders of **3b** decompose above 245 °C.

The UV-vis absorption band of **3b** (recorded in THF) at 402 nm. Compound **3b** is comparatively more soluble in THF than **3a**.

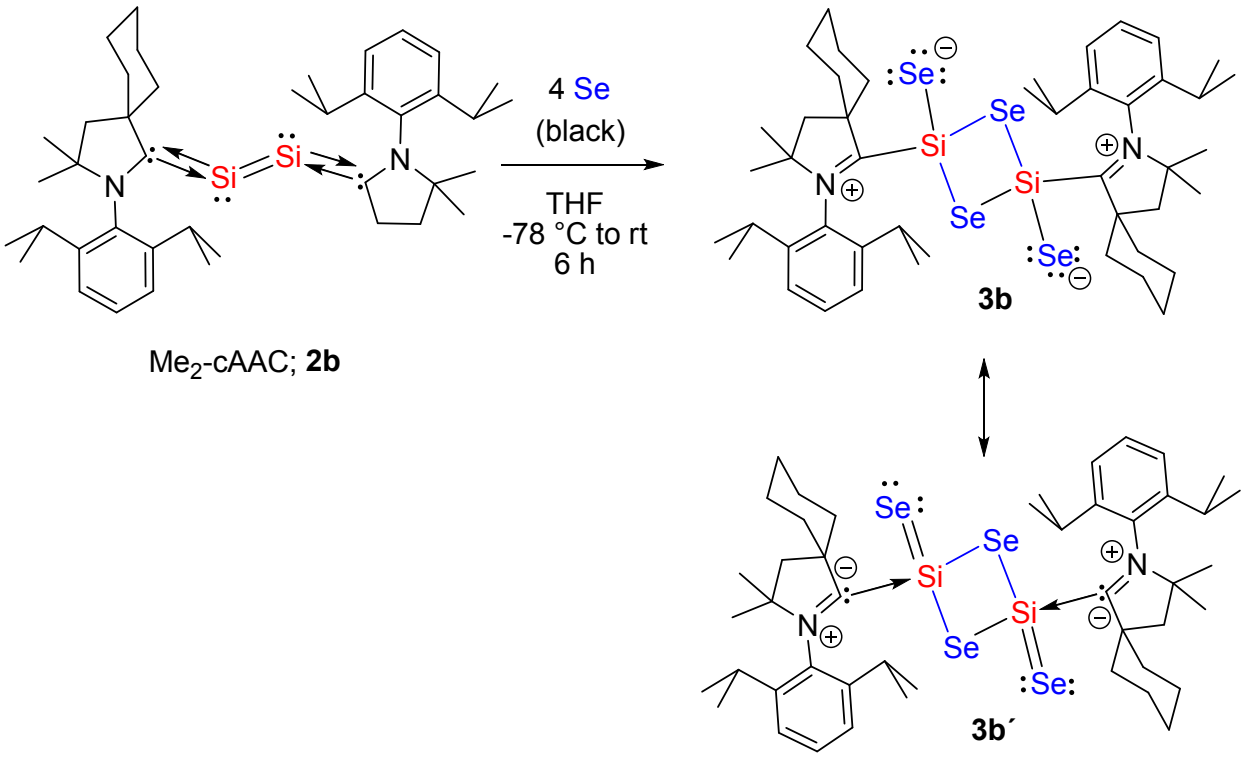

Scheme S4: Synthesis of compound **3b** from **2b**.

Common observations for **3a-b**: The crystals of **3a-b** are stable in air for several days and retain their dark orange color for a week while THF solutions of **3a-b** slowly loose their colors when exposed to air. The powders of **3a-b** are relatively less stable in air when compared with those of their crystals. Compounds **3a-b** have a strong smell which is common for selenium containing organic compounds. Both the compounds **3a-b** are studied by solution and solid state NMR measurements. ^{1}H and ^{13}C NMR resonances are very broad (both in solid state and in solution) and hence not much informative. ^{29}Si and ^{77}Se NMR resonances are not observed. However, the corresponding chemical shift values of carbene carbon, silicon, and selenium atoms are theoretically calculated and given in the theoretical part.

(S2) UV-visible spectroscopy

UV-vis spectra were recorded on Varian Cary 5000 (Varian) spectrophotometer.

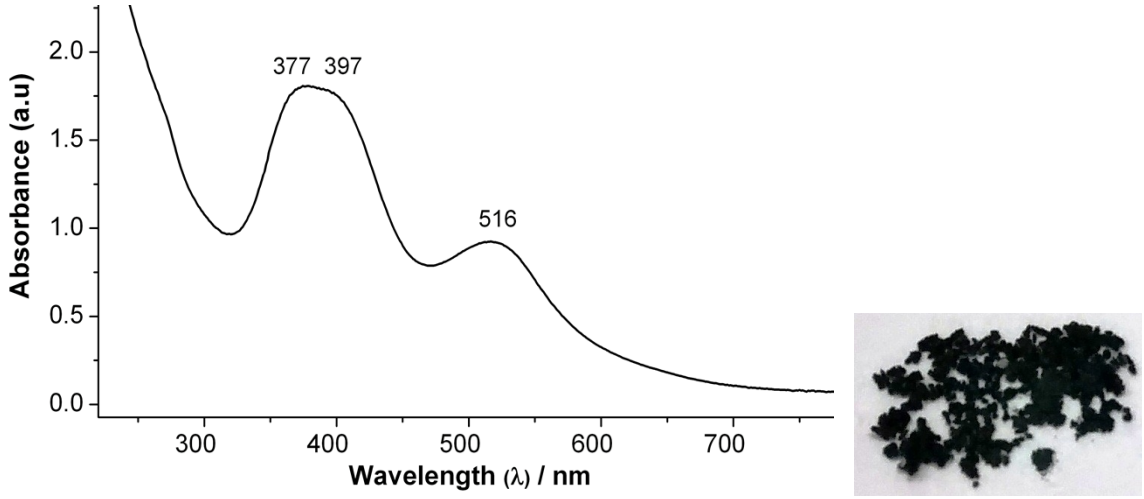

Figure S1. UV-visible spectrum of compound **2a** in *n*-hexane (left). Solid sample of **2a** (right). When these crystals are dissolved in organic solvents dark purple color solutions are obtained.

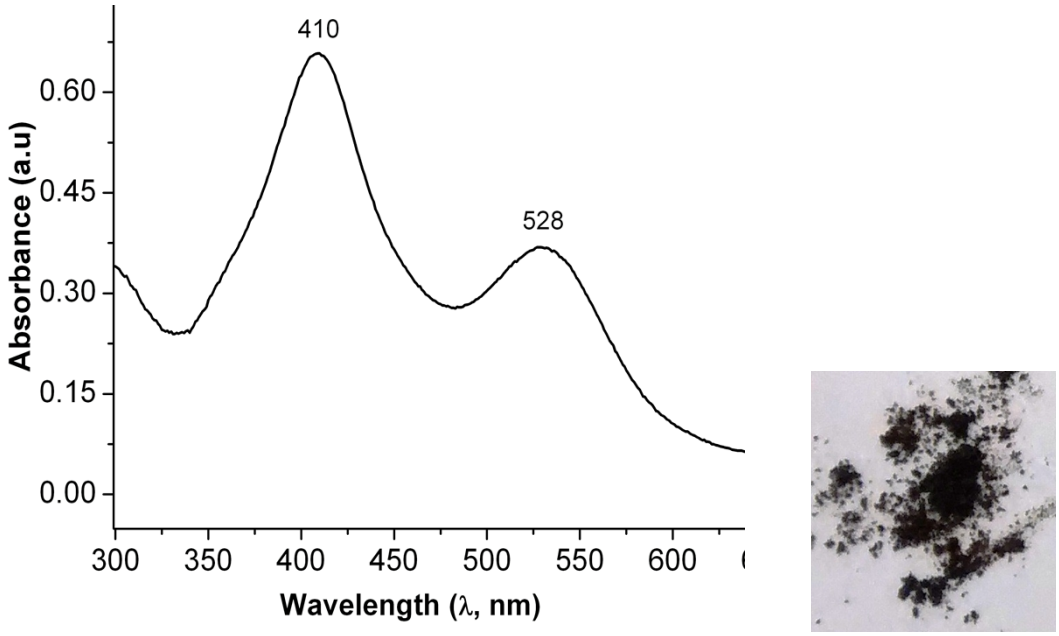

Figure S2. UV-visible spectrum of compound **2b** in *n*-hexane (left). Solid powdered sample of **2b** (right).

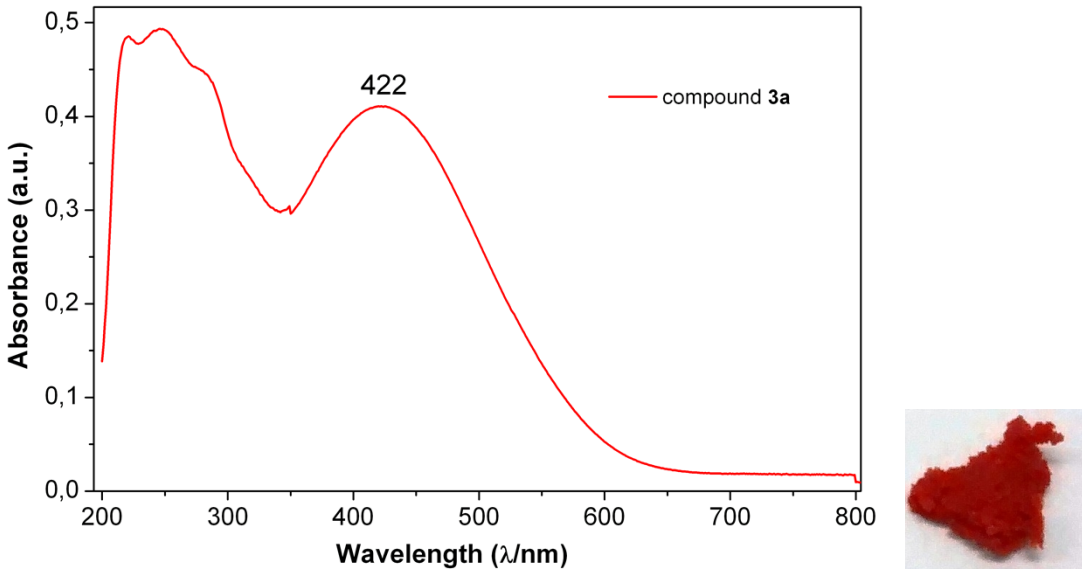

Figure S3. UV-visible spectrum of solid powered sample of compound **3a** (left). Solid sample of **3a** (right).

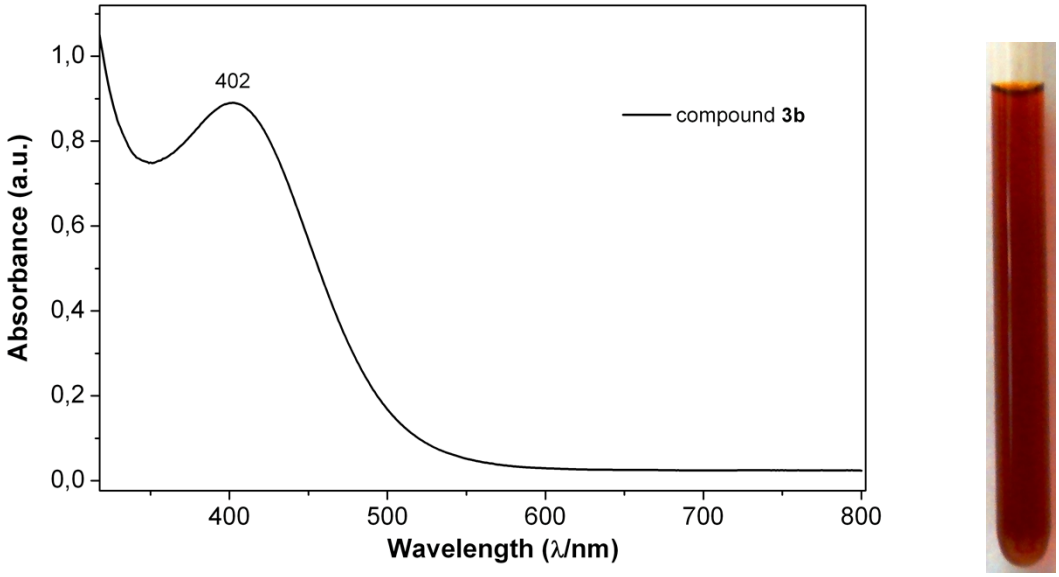

Figure S4. UV-visible spectrum of compound **3b** in THF (left). THF solution of **3b** (right).

(S3) Crystal data

The molecular structures of **2a**, and **2b** were elucidated by single-crystal X-ray diffraction. Crystallographic data for **2a-b, 3a·2THF,** and Me_2-cAAC=O[S5] were measured on a Bruker three-circle diffractometer equipped with a SMART 6000 CCD area detector and a CuK alpha rotating anode. Integrations were performed with SAINT 8.27B. Intensity data for all three compounds were corrected for absorption and scaled with SADABS.[S6] Synchrotron data from XDS integration were converted with XDS2SAD (G. Sheldrick) prior to use with SADABS. All crystals were measured at a temperature of 100 K. Structures were solved by direct methods and those of **2a** and **2b** refined by full-matrix least-squares methods on F^2 with the program SHELXL12[S7] using anisotropic displacement parameters for all non-hydrogen atoms. Anomalous dispersion for the chosen wavelength was adjusted with the DISP command for the synchroton data. Unmerged intensity data and the SHELXL refinement instructions are included in the respective CIF files.

Data for Me_2-cAAC=O were refined with aspherical scattering factors of the invariom database.[S8] Invariom refinement led to an improvement in the crystallographic R-factor of 1.27 %. Refinement was carried out with XDLSM from the XD suite of programs.[S9]

The X-ray diffraction study on black needle shaped single crystals of compounds $(Me_2\text{-cAAC})_2Si_2$ (**2a**) and $(Cy\text{-cAAC})_2Si_2$ (**2b**) show that both crystallize in the triclinic space group *P*-1. The crystal data of both **2a** and **2b** were collected at 100 K. Structural analysis of **2** shows silicon atoms are disordered. The structure analysis exhibits that only half of the molecule is contained in the asymmetric unit.

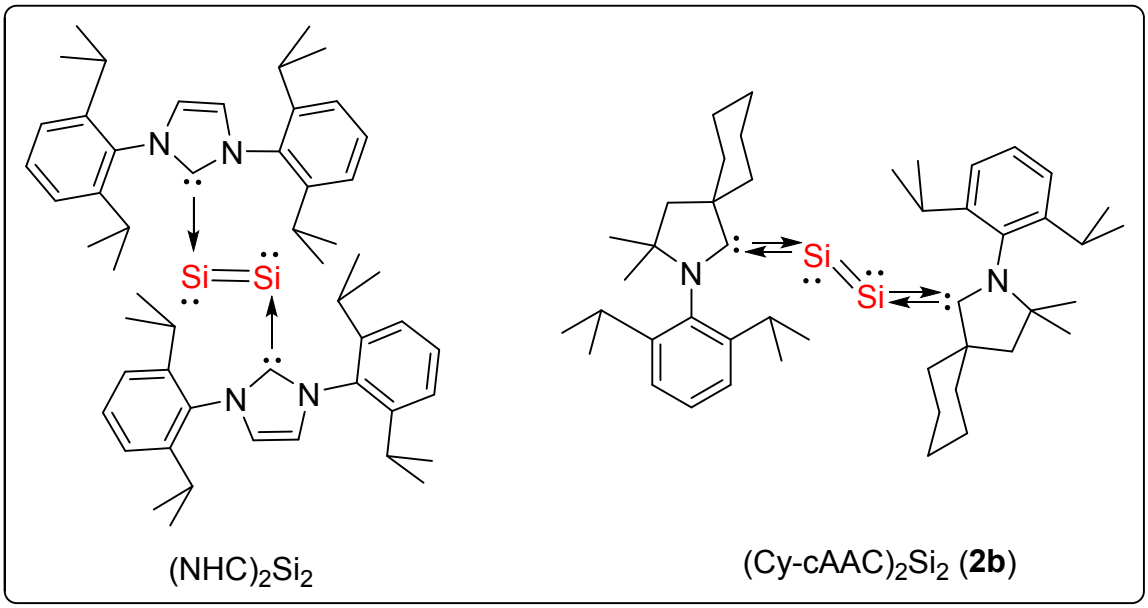

Scheme S5: The bond between NHC and Si_2 is a strong σ-donor type (C_{NHC}→Si) with negligible back bonding (left). The bond between cAAC and Si_2 in $(Cy\text{-cAAC})_2Si_2$ (**2b**) is a strong σ-donor type (C_{NHC}→Si) with strong π-back donation from C_{cAAC} to Si_2 (C_{cAAC}←Si) (right). Thus the bond between C_{cAAC} and silicon atoms has partial

double bond character. The electronic structure of (Cy-cAAC)$_2$Si$_2$ (**2b**) was concluded as shown in Scheme S5. It is arranged from combined Raman spectroscopy and theoretical calculation.[S3]

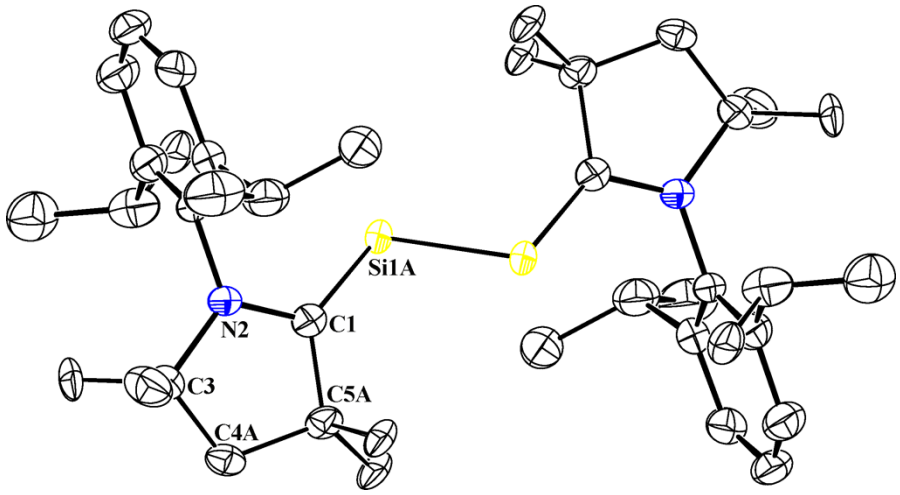

Figure S5. Molecular structure of **2a** (ORTEP picture with 50% probability), hydrogen atoms were omitted for clarity. (T = 100 K) (major conformer 75%)

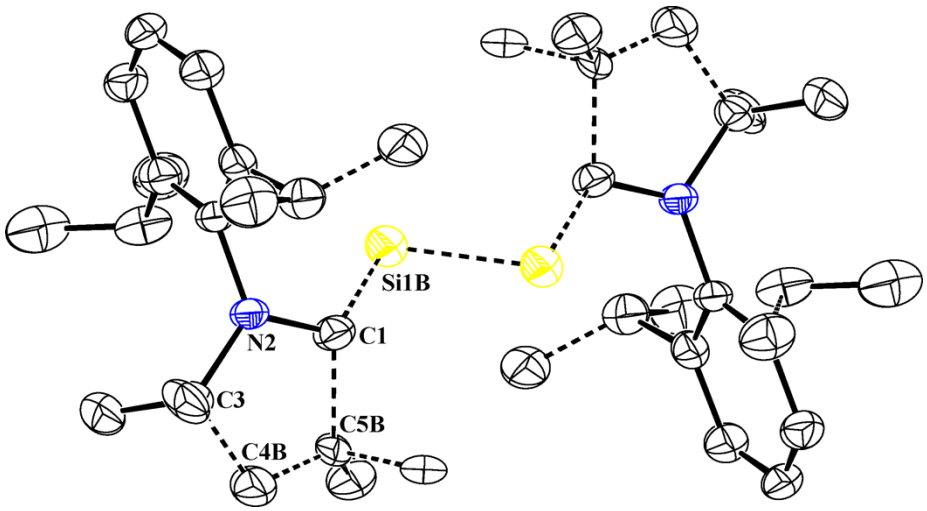

Figure S6. Representation of molecular structure of disordered part **2a** (ORTEP picture with 50% probability), hydrogen atoms were removed for clarity. (T = 100 K) (minor conformer 25 %). Figures S5 and S6 suggests that the Me$_2$-cAAC carbene in **2a** is evenly disordered in solid state.

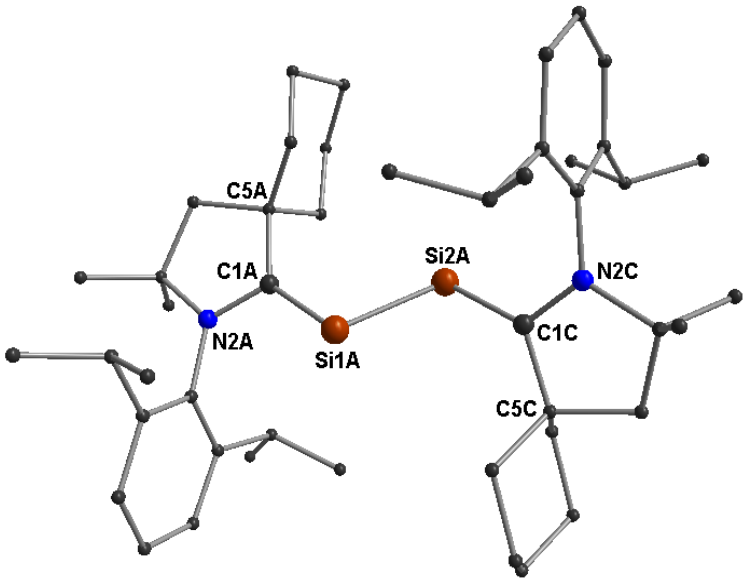

Figure S7. Molecular structure of (Cy-cAAC)$_2$Si$_2$ (**2b**). Hydrogen atoms were omitted for clarity. (T = 100 K)

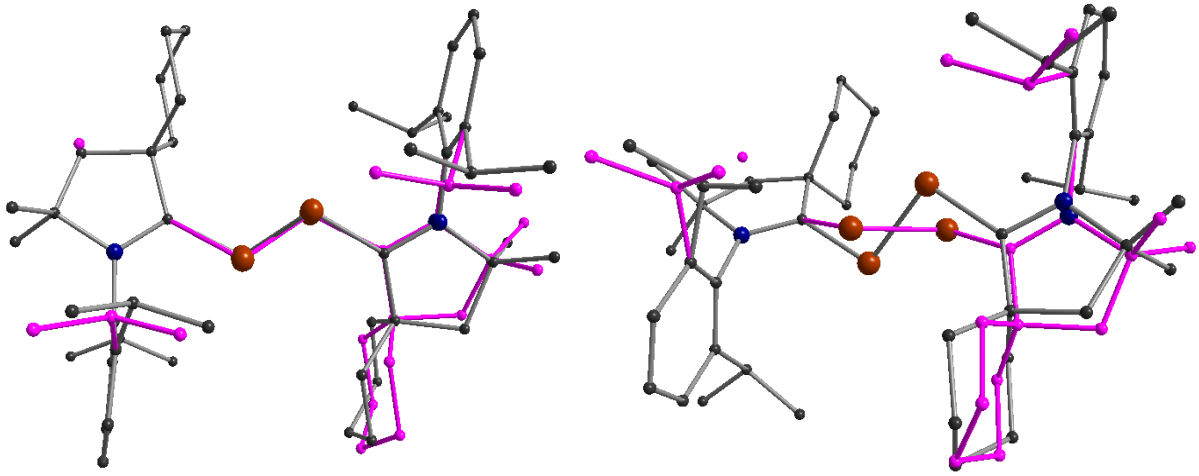

Figure S8. Different views on molecular structures of two conformers of **2b** (major in grey; minor in purple) in solid state. The picture at the right hand side shows that the Cy-cAAC carbene (colored in purple) is disordered. The occupancy ratio of grey:purple part is 80:20 at 100 K and ~ 97:3 at 23 K. Figures S7 and S8 suggests that the Cy-cAAC carbene in **2b** is unevenly disordered in solid state.

Table S1. Selected bond parameters of $(Me_2\text{-cAAC})_2Si_2$ (**2a**) and $(Me_2\text{-cAAC})_2Si_2Se_4\cdot 2THF$ (**3a·2THF**).

Compound	**2a** (at 100 K)	**2b** (at 23 K)[S3]	**2b** (at 100 K)	$(NHC)_2Si_2$ [S10]
Si-$C_{carbene}$ (Å)	1.887(4)	1.849(4)-1.876(4)	1.836(18), 1.878(5), 1.861(4)	1.9271(15)
$C_{carbene}$ -N	1.342(5)	1.352(3)	1.33(2)-1.347(6)	-
Si-Si (Å)	2.232(9)/2.254(2)	2.254(3)	2.232 (9)-2.255(4)	2.2294(11)
C1-Si1-Si2/C21-Si1-Si2 (°)	103.67(14)	101.22 (13)/ 105.14(13)	101.99(14), 104.24(12), 105.1(6), 97.9(3)	93.37(5)
C1-Si1-Si2-C21 (°)	180.0	179.16	179.03	180.0
Center of inversion between two silicon atoms	yes	yes	No	yes
……..	.....	.....	.....	.....
Compound	**2a** (at 100 K)	**1a** [S2]	**3a**	
Si-$C_{carbene}$ (Å)	1.887(4)	1.944(2)	1.931(4)	
$C_{carbene}$ -N	1.342(5)	1.303 (2)	1.311(5)	
Si-Si (Å)	2.232(9)/2.254(2)	-	3.056	
C-$C_{carbene}$ –N (°)	105.9(19)/109.0(7)	110.1 (4)	110.0 (3)	

Table S2. Crystal data and structure refinement of $(Me_2\text{-cAAC})_2Si_2$ (**2a**) and $(Me_2\text{-cAAC})_2Si_2Se_4\cdot 2THF$ (**3a·2THF**).

Compound	$(Me_2\text{-cAAC})_2Si_2$ (Me_2-cAAC = :C(CH_2)(CMe_2)$_2$N-2,6-*i*$Pr_2C_6H_3$) (**2a**)	$(Me_2\text{-cAAC})_2Si_2Se_4$ (Me_2-cAAC = :C(CH_2)(CMe_2)$_2$N-2,6-*i*$Pr_2C_6H_3$) (**3a·2THF**)
Empirical formula	$C_{40}H_{62}N_2Si_2$	$C_{20}H_{31}NSe_2Si\cdot(C_4H_8O)$
CCDC no.	926618	1060365
Molecular weight	627.09	543.57
Crystal size [mm]	0.02 x 0.01 x 0.01	0.09 x 0.08 x 0.06
Wavelength [Å]	1.54178	1.54178
Crystal system	triclinic	monoclinic,
Space group	*P*-1	$P2_1/n$
a [Å]	9.4109(9)	14.6952 (6)
b [Å]	10.1841(10)	10.0800 (4)

c [Å]	11.6538(12)	17.7472 (7)
α [°]	91.036(6)	90.0
β [°]	102.694(6)	109.567 (2)
γ [°]	116.006(6)	90.0
V [Å ^{3}]	970.92(17)	2477.03 (17)
Z	1	4
Temperature [K]	100(2)	100(2)
ρ [Mg m^{-3}]	1.073	1.458
μ [mm^{-1}]	1.02	4.30
F (000)	344	1120
θ-area [°]	3.9 to 65.2	3.4 to 70.1
Total number reflect.	16983	22159
Unique reflections	3341	4611
reflections with $I > 2\sigma(I)$	2685	3674
R_{int}	0.0645	0.062
Number of restraints	130	264
Parameters	276	301
$R1$ [$I>2\sigma(I)$]	0.0747	0.0393
$wR2$ [$I>2\sigma(I)$]	0.1935	0.0922
$R1$ [all data]	0.0908	0.0556
$wR2$ [all data]	0.2049	0.1002
GooF	1.064	1.02
Extinction coefficient		
Largest diff. peak / hole		
max. / min. [10^3·e·nm $^{-3}$]	0.452 and -0.276	1.01 and −0.42

Table S3. Crystal data and structure refinement of (Cy-cAAC:)$_2$Si$_2$ (**2b**) at two different temperatures (23 K[S1] and 100 K).

Compound	(Cy-cAAC:)$_2$Si$_2$ (Cy-cAAC: = :C(CH_2)(CMe_2)(C_6H_{10})N-2,6-*i*Pr$_2$C$_6$H$_3$) (**2b**) at T = 23 K[S3]	2 (Cy-cAAC:)$_2$Si$_2$ (Cy-cAAC: = :C(CH_2)(CMe_2)(C_6H_{10})N-2,6-*i*Pr$_2$C$_6$H$_3$) (**2b**) at T =100 K
Empirical formula	$C_{46}H_{70}N_2Si_2$	$C_{92}H_{140}N_4Si_4$
CCDC no.	983863	948799
Molecular weight	707.22	1414.43
Crystal size [mm]	0.07 × 0.03 × 0.02	0.04 × 0.01 × 0.01
Wavelength [Å]	0.4769	0.6358
Crystal system	triclinic	triclinic
Space group	*P*-1	*P*-1
a [Å]	12.79(2)	12.80(3)
b [Å]	13.783(9)	13.86(4)
c [Å]	14.433(19)	14.36(2)
α [°]	66.35(6)	66.45(7)
β [°]	79.58(10)	79.90(4)
γ [°]	67.48(7)	67.84(9)

V [nm^3]	2152(5)	2162(8)
Z	2	2
Temperature [K]	23	100
ρ [Mg m^{-3}]	1.091	1.086
μ [mm^{-1}]	0.06	0.09
F (000)	776	776
θ-area [°]	1.0 to 16.9	2.0 to 22.6
Total number reflect.	45604	24747
Unique reflections	7928	7289
reflections with $I > 2\sigma(I)$	4507	5848
R_{int}	-	0.080
Number of restraints	18	238
Parameters	493	635
$R1$ [$I>2\sigma(I)$]	0.0641	0.0692
$wR2$ [$I>2\sigma(I)$]	0.1418	0.1814
$R1$ [all data]	0.1285	0.0843
$wR2$ [all data]	0.1721	0.1930
GooF	1.03	1.031
Extinction coefficient		
Largest diff. peak / hole max. / min. [10^3·e·nm^{-3}]	0.31 and -0.31	0.485 and -0.335

See Reference S3 for single crystal X-ray data of compound **2b** at 23 K. It is given here for proper comparison.

Table S4. Bond lengths [Å] and angles [°] for $(Me_2\text{-cAAC})_2Si_2$ (**2a**).

Si1A—C1	1.887 (4)	C4B—C5B	1.48 (6)
Si1A—Si1A^i	2.254 (2)	C5B—C9B	1.42 (5)
Si1B—C1	1.978 (6)	C5B—C8B	1.51 (5)
Si1B—Si1B^i	2.232 (9)	C10—C15	1.406 (5)
C1—N2	1.342 (5)	C10—C11	1.416 (5)
C1—C5A	1.502 (15)	C11—C12	1.395 (5)
C1—C5B	1.64 (5)	C11—C16	1.520 (5)
N2—C10	1.453 (4)	C12—C13	1.375 (6)
N2—C3	1.504 (4)	C13—C14	1.372 (6)
C3—C6B	1.31 (4)	C14—C15	1.395 (5)
C3—C7	1.517 (6)	C15—C19	1.527 (6)

C3—C4A	1.534 (8)	C16—C17	1.521 (7)
C3—C4B	1.56 (3)	C16—C18B	1.53 (2)
C3—C6A	1.568 (10)	C16—C18A	1.561 (8)
C4A—C5A	1.546 (18)	C19—C21A	1.527 (7)
C5A—C8A	1.532 (15)	C19—C20	1.53.0 (6)
C5A—C9A	1.567 (12)	C19—C21B	1.64 (2)
C1—Si1A—Si1A^{i}	103.67 (14)	C5B—C4B—C3	109 (3)
C1—Si1B—Si1B^{i}	98.9 (3)	C9B—C5B—C4B	123 (3)
N2—C1—C5A	109.0 (7)	C9B—C5B—C8B	108 (4)
N2—C1—C5B	105.9 (19)	C4B—C5B—C8B	104 (4)
N2—C1—Si1A	122.6 (3)	C9B—C5B—C1	119 (4)
C5A—C1—Si1A	126.3 (6)	C4B—C5B—C1	104 (3)
N2—C1—Si1B	119.7 (3)	C8B—C5B—C1	95 (2)
C5B—C1—Si1B	118 (2)	C15—C10—C11	120.8 (3)
C1—N2—C10	121.9 (3)	C15—C10—N2	120.3 (3)
C1—N2—C3	115.5 (3)	C11—C10—N2	118.9 (3)
C10—N2—C3	122.6 (3)	C12—C11—C10	118.1 (3)
C6B—C3—N2	112.8 (19)	C12—C11—C16	118.7 (4)
C6B—C3—C7	116.9 (18)	C10—C11—C16	123.1 (3)
N2—C3—C7	112.2 (3)	C13—C12—C11	121.3 (4)
N2—C3—C4A	99.8 (4)	C14—C13—C12	120.0 (4)
C7—C3—C4A	116.5 (4)	C13—C14—C15	121.7 (4)
C6B—C3—C4B	112 (2)	C14—C15—C10	118.0 (4)
N2—C3—C4B	102.9 (12)	C14—C15—C19	117.5 (3)
C7—C3—C4B	98.2 (11)	C10—C15—C19	124.5 (3)
N2—C3—C6A	111.5 (6)	C11—C16—C17	111.5 (4)
C7—C3—C6A	106.9 (5)	C11—C16—C18B	122.7 (9)

C4A—C3—C6A	110.0 (5)	C17—C16—C18B	88.1 (9)
C3—C4A—C5A	107.5 (7)	C11—C16—C18A	107.8 (4)
C1—C5A—C8A	118.4 (8)	C17—C16—C18A	114.6 (4)
C1—C5A—C4A	102.4 (9)	C15—C19—C21A	113.0 (4)
C8A—C5A—C4A	111.2 (10)	C15—C19—C20	112.1 (3)
C1—C5A—C9A	105.4 (9)	C21A—C19—C20	105.0 (4)
C8A—C5A—C9A	108.6 (10)	C15—C19—C21B	100.6 (8)
C4A—C5A—C9A	110.5 (7)	C20—C19—C21B	129.6 (8)

Symmetry code: (i) –x+1, -y+2, -z+1.

Table S5. Bond lengths [Å] and angles [°] for (Cy-cAAC)$_2$Si$_2$ (**2b**) (at T = 100 K).

Si1A—C1A	1.878 (5)	C16A—C17A	1.372 (5)
Si1A—Si2A	2.255 (4)	C17A—C18A	1.397 (5)
Si2A—C1C	1.861 (4)	C18A—C19A	1.517 (5)
Si1C—C1B	1.836 (18)	C19A—C20A	1.519 (6)
Si1C—Si2C	2.232 (9)	C19A—C21A	1.544 (5)
Si2C—C1C	2.016 (6)	C22A—C24A	1.535 (6)
C1A—N2A	1.347 (6)	C22A—C23A	1.541 (6)
C1A—C5A	1.534 (6)	C22B—C23B	1.541 (10)
N2A—C13A	1.440 (5)	C22B—C24B	1.549 (10)
N2A—C3A	1.512 (7)	C1C—N2C	1.349 (5)
C3A—C7A	1.525 (6)	C1C—C5C	1.527 (5)
C3A—C4A	1.533 (7)	N2C—C13C	1.445 (4)
C3A—C6A	1.537 (6)	N2C—C3C	1.506 (4)
C4A—C5A	1.532 (6)	C3C—C7C	1.503 (5)
C5A—C12A	1.538 (7)	C3C—C6C	1.513 (5)
C5A—C8A	1.549 (10)	C3C—C4D	1.516 (13)
C8A—C9A	1.540 (6)	C3C—C4C	1.568 (10)
C9A—C10A	1.520 (7)	C4C—C5C	1.550 (7)
C10A—C11A	1.535 (7)	C4D—C5C	1.610 (10)
C11A—C12A	1.536 (6)	C5C—C12C	1.521 (5)
C1B—N2B	1.33 (2)	C5C—C8C	1.524 (6)

C1B—C5B	1.56 (3)	C8C—C9C	1.549 (6)
N2B—C3B	1.50 (3)	C9C—C10C	1.479 (6)
N2B—C13A	1.58 (2)	C10C—C11C	1.493 (6)
C3B—C4B	1.48 (3)	C11C—C12C	1.525 (5)
C3B—C6B	1.516 (11)	C13C—C18C	1.400 (5)
C3B—C7B	1.525 (10)	C13C—C14C	1.413 (5)
C4B—C5B	1.60 (3)	C14C—C15C	1.406 (5)
C5B—C8B	1.44 (4)	C14C—C22C	1.518 (5)
C5B—C12B	1.543 (11)	C15C—C16C	1.368 (5)
C8B—C9B	1.540 (10)	C16C—C17C	1.375 (5)
C9B—C10B	1.530 (11)	C17C—C18C	1.405 (5)
C10B—C11B	1.535 (10)	C18C—C19D	1.523 (10)
C11B—C12B	1.542 (10)	C18C—C19C	1.527 (5)
C13A—C14A	1.404 (5)	C19C—C20C	1.531 (7)
C13A—C18A	1.416 (5)	C19C—C21C	1.550 (7)
C14A—C15A	1.400 (5)	C19D—C20D	1.52 (4)
C14A—C22A	1.517 (5)	C19D—C21D	1.60 (3)
C14A—C22B	1.542 (10)	C22C—C23C	1.533 (5)
C15A—C16A	1.372 (5)	C22C—C24C	1.536 (5)
C1A—Si1A—Si2A	101.99 (14)	C13A—C18A—C19A	123.8 (3)
C1C—Si2A—Si1A	104.24 (12)	C18A—C19A—C20A	113.9 (3)
C1B—Si1C—Si2C	105.1 (6)	C18A—C19A—C21A	109.1 (3)
C1C—Si2C—Si1C	97.9 (3)	C20A—C19A—C21A	109.8 (3)
N2A—C1A—C5A	107.9 (3)	C14A—C22A—C24A	110.5 (3)
N2A—C1A—Si1A	119.3 (3)	C14A—C22A—C23A	113.3 (4)
C5A—C1A—Si1A	132.3 (3)	C24A—C22A—C23A	108.2 (4)
C1A—N2A—C13A	123.5 (3)	C23B—C22B—C14A	108.1 (15)
C1A—N2A—C3A	115.7 (4)	C23B—C22B—C24B	110.9 (18)
C13A—N2A—C3A	120.6 (4)	C14A—C22B—C24B	113.6 (15)
N2A—C3A—C7A	112.1 (5)	N2C—C1C—C5C	108.8 (2)
N2A—C3A—C4A	100.7 (4)	N2C—C1C—Si2A	124.5 (2)
C7A—C3A—C4A	112.1 (4)	C5C—C1C—Si2A	124.8 (3)
N2A—C3A—C6A	111.0 (4)	N2C—C1C—Si2C	111.1 (3)
C7A—C3A—C6A	109.1 (5)	C5C—C1C—Si2C	133.3 (3)
C4A—C3A—C6A	111.7 (4)	C1C—N2C—C13C	122.3 (2)

C5A—C4A—C3A	107.7 (4)	C1C—N2C—C3C	115.7 (2)
C4A—C5A—C1A	104.0 (3)	C13C—N2C—C3C	122.0 (3)
C4A—C5A—C12A	111.6 (4)	C7C—C3C—N2C	110.9 (3)
C1A—C5A—C12A	112.8 (4)	C7C—C3C—C6C	108.7 (3)
C4A—C5A—C8A	112.0 (4)	N2C—C3C—C6C	111.5 (3)
C1A—C5A—C8A	108.4 (4)	C7C—C3C—C4D	97.7 (6)
C12A—C5A—C8A	108.1 (4)	N2C—C3C—C4D	102.1 (4)
C9A—C8A—C5A	113.3 (6)	C6C—C3C—C4D	124.9 (6)
C10A—C9A—C8A	111.2 (6)	C7C—C3C—C4C	121.9 (6)
C9A—C10A—C11A	111.6 (5)	N2C—C3C—C4C	100.8 (3)
C10A—C11A—C12A	109.8 (4)	C6C—C3C—C4C	102.6 (5)
C11A—C12A—C5A	112.1 (4)	C5C—C4C—C3C	106.2 (5)
N2B—C1B—C5B	108.8 (15)	C3C—C4D—C5C	105.8 (7)
N2B—C1B—Si1C	127.1 (14)	C12C—C5C—C8C	108.7 (3)
C5B—C1B—Si1C	120.9 (12)	C12C—C5C—C1C	110.7 (2)
C1B—N2B—C3B	117.5 (17)	C8C—C5C—C1C	110.7 (3)
C1B—N2B—C13A	122.8 (15)	C12C—C5C—C4C	120.1 (5)
C3B—N2B—C13A	118.3 (14)	C8C—C5C—C4C	101.9 (5)
C4B—C3B—N2B	101.0 (16)	C1C—C5C—C4C	104.3 (4)
C4B—C3B—C6B	115.7 (19)	C12C—C5C—C4D	98.3 (6)
N2B—C3B—C6B	109.1 (18)	C8C—C5C—C4D	125.3 (6)
C4B—C3B—C7B	115 (2)	C1C—C5C—C4D	102.2 (5)
N2B—C3B—C7B	109 (2)	C5C—C8C—C9C	111.4 (3)
C6B—C3B—C7B	107 (2)	C10C—C9C—C8C	111.7 (3)
C3B—C4B—C5B	110.3 (17)	C9C—C10C—C11C	112.2 (4)
C8B—C5B—C12B	116 (2)	C10C—C11C—C12C	111.3 (3)
C8B—C5B—C1B	119.7 (18)	C5C—C12C—C11C	112.3 (3)
C12B—C5B—C1B	103.9 (15)	C18C—C13C—C14C	120.9 (3)
C8B—C5B—C4B	109 (2)	C18C—C13C—N2C	120.0 (3)
C12B—C5B—C4B	106.0 (18)	C14C—C13C—N2C	119.1 (3)
C1B—C5B—C4B	99.9 (15)	C15C—C14C—C13C	117.8 (3)
C5B—C8B—C9B	112 (3)	C15C—C14C—C22C	117.7 (3)
C10B—C9B—C8B	111 (3)	C13C—C14C—C22C	124.4 (3)
C9B—C10B—C11B	113 (3)	C16C—C15C—C14C	121.5 (3)
C10B—C11B—C12B	108 (3)	C15C—C16C—C17C	119.8 (3)
C11B—C12B—C5B	115 (2)	C16C—C17C—C18C	121.6 (3)

C14A—C13A—C18A	121.6 (3)	C13C—C18C—C17C	117.9 (3)
C14A—C13A—N2A	117.1 (3)	C13C—C18C—C19D	133.7 (12)
C18A—C13A—N2A	121.3 (3)	C17C—C18C—C19D	107.3 (12)
C14A—C13A—N2B	133.8 (6)	C13C—C18C—C19C	122.3 (4)
C18A—C13A—N2B	104.5 (7)	C17C—C18C—C19C	119.6 (4)
C15A—C14A—C13A	117.4 (3)	C18C—C19C—C20C	111.3 (5)
C15A—C14A—C22A	116.8 (3)	C18C—C19C—C21C	109.4 (5)
C13A—C14A—C22A	125.7 (3)	C20C—C19C—C21C	108.1 (4)
C15A—C14A—C22B	130.5 (10)	C20D—C19D—C18C	113 (2)
C13A—C14A—C22B	110.1 (10)	C20D—C19D—C21D	109.1 (19)
C16A—C15A—C14A	121.5 (3)	C18C—C19D—C21D	119.2 (19)
C15A—C16A—C17A	120.5 (3)	C14C—C22C—C23C	112.9 (3)
C16A—C17A—C18A	121.3 (3)	C14C—C22C—C24C	110.4 (3)
C17A—C18A—C13A	117.4 (3)	C23C—C22C—C24C	108.1 (3)
C17A—C18A—C19A	118.5 (3)		

Table S6. Bond lengths [Å] and angles [°] for $(Me_2\text{-cAAC})_2Si_2Se_4 \cdot 2THF$ (**3a·2THF**)

Se2—Si1	2.1510 (10)	C17—H17A	0.9800
Se1—Si1	2.2874 (10)	C17—H17B	0.9800
Se1—Si1^{i}	2.3045 (10)	C17—H17C	0.9800
Si1—C1	1.931 (4)	C18—C20	1.525 (5)
Si1—Se1^{i}	2.3046 (10)	C18—C19	1.538 (5)
N1—C1	1.311 (5)	C18—H18	1.0000
N1—C9	1.464 (5)	C19—H19A	0.9800
N1—C4	1.540 (4)	C19—H19B	0.9800
C1—C2	1.528 (5)	C19—H19C	0.9800
C2—C3A	1.516 (8)	C20—H20A	0.9800
C2—C5	1.521 (6)	C20—H20B	0.9800
C2—C6	1.527 (6)	C20—H20C	0.9800
C2—C3B	1.599 (12)	C3A—H3A	0.9900
C4—C3B	1.410 (13)	C3A—H3B	0.9900
C4—C8A	1.444 (8)	C7A—H7AA	0.9800
C4—C7B	1.469 (12)	C7A—H7AB	0.9800
C4—C3A	1.555 (9)	C7A—H7AC	0.9800
C4—C7A	1.615 (8)	C8A—H8A1	0.9800

C4—C8B	1.650 (12)	C8A—H8A2	0.9800
C5—H5A	0.9800	C8A—H8A3	0.9800
C5—H5B	0.9800	C3B—H3B1	0.9900
C5—H5C	0.9800	C3B—H3B2	0.9900
C6—H6A	0.9800	C7B—H7BA	0.9800
C6—H6B	0.9800	C7B—H7BB	0.9800
C6—H6C	0.9800	C7B—H7BC	0.9800
C9—C10	1.407 (5)	C8B—H8B1	0.9800
C9—C14	1.410 (5)	C8B—H8B2	0.9800
C10—C11	1.401 (6)	C8B—H8B3	0.9800
C10—C15	1.525 (5)	O5T_1—C1T_1	1.395 (8)
C11—C12	1.377 (6)	O5T_1—C4T_1	1.411 (7)
C11—H11	0.9500	C1T_1—C2T_1	1.453 (8)
C12—C13	1.384 (6)	C1T_1—H1TA_1	0.9900
C12—H12	0.9500	C1T_1—H1TB_1	0.9900
C13—C14	1.386 (5)	C2T_1—C3T_1	1.478 (9)
C13—H13	0.9500	C2T_1—H2TA_1	0.9900
C14—C18	1.522 (5)	C2T_1—H2TB_1	0.9900
C15—C16	1.527 (5)	C3T_1—C4T_1	1.503 (8)
C15—C17	1.528 (6)	C3T_1—H3TA_1	0.9900
C15—H15	1.0000	C3T_1—H3TB_1	0.9900
C16—H16A	0.9800	C4T_1—H4TA_1	0.9900
C16—H16B	0.9800	C4T_1—H4TB_1	0.9900
C16—H16C	0.9800		
Si1—Se1—Si1^{i}	83.45 (4)	H17B—C17—H17C	109.5
C1—Si1—Se2	97.86 (11)	C14—C18—C20	110.0 (3)
C1—Si1—Se1	113.81 (11)	C14—C18—C19	112.3 (3)
Se2—Si1—Se1	120.35 (4)	C20—C18—C19	110.1 (3)
C1—Si1—Se1^{i}	109.85 (11)	C14—C18—H18	108.1
Se2—Si1—Se1^{i}	119.05 (4)	C20—C18—H18	108.1
Se1—Si1—Se1^{i}	96.55 (4)	C19—C18—H18	108.1
C1—N1—C9	125.6 (3)	C18—C19—H19A	109.5
C1—N1—C4	113.2 (3)	C18—C19—H19B	109.5
C9—N1—C4	121.0 (3)	H19A—C19—H19B	109.5
N1—C1—C2	110.0 (3)	C18—C19—H19C	109.5
N1—C1—Si1	126.9 (3)	H19A—C19—H19C	109.5

C2—C1—Si1	122.3 (3)	H19B—C19—H19C	109.5
C3A—C2—C5	120.1 (5)	C18—C20—H20A	109.5
C3A—C2—C6	103.4 (5)	C18—C20—H20B	109.5
C5—C2—C6	107.1 (4)	H20A—C20—H20B	109.5
C3A—C2—C1	102.9 (4)	C18—C20—H20C	109.5
C5—C2—C1	107.8 (3)	H20A—C20—H20C	109.5
C6—C2—C1	116.0 (3)	H20B—C20—H20C	109.5
C5—C2—C3B	98.1 (6)	C2—C3A—C4	106.4 (5)
C6—C2—C3B	125.5 (6)	C2—C3A—H3A	110.5
C1—C2—C3B	100.1 (5)	C4—C3A—H3A	110.5
C3B—C4—C7B	124.1 (8)	C2—C3A—H3B	110.5
C3B—C4—N1	101.3 (5)	C4—C3A—H3B	110.5
C8A—C4—N1	112.7 (4)	H3A—C3A—H3B	108.6
C7B—C4—N1	111.7 (5)	C4—C7A—H7AA	109.5
C8A—C4—C3A	115.7 (5)	C4—C7A—H7AB	109.5
N1—C4—C3A	101.1 (4)	H7AA—C7A—H7AB	109.5
C8A—C4—C7A	107.4 (5)	C4—C7A—H7AC	109.5
N1—C4—C7A	110.3 (4)	H7AA—C7A—H7AC	109.5
C3A—C4—C7A	109.5 (5)	H7AB—C7A—H7AC	109.5
C3B—C4—C8B	107.8 (8)	C4—C8A—H8A1	109.5
C7B—C4—C8B	106.6 (7)	C4—C8A—H8A2	109.5
N1—C4—C8B	103.6 (5)	H8A1—C8A—H8A2	109.5
C2—C5—H5A	109.5	C4—C8A—H8A3	109.5
C2—C5—H5B	109.5	H8A1—C8A—H8A3	109.5
H5A—C5—H5B	109.5	H8A2—C8A—H8A3	109.5
C2—C5—H5C	109.5	C4—C3B—C2	109.5 (8)
H5A—C5—H5C	109.5	C4—C3B—H3B1	109.8
H5B—C5—H5C	109.5	C2—C3B—H3B1	109.8
C2—C6—H6A	109.5	C4—C3B—H3B2	109.8
C2—C6—H6B	109.5	C2—C3B—H3B2	109.8
H6A—C6—H6B	109.5	H3B1—C3B—H3B2	108.2
C2—C6—H6C	109.5	C4—C7B—H7BA	109.5
H6A—C6—H6C	109.5	C4—C7B—H7BB	109.5
H6B—C6—H6C	109.5	H7BA—C7B—H7BB	109.5
C10—C9—C14	121.6 (3)	C4—C7B—H7BC	109.5
C10—C9—N1	121.5 (3)	H7BA—C7B—H7BC	109.5

C14—C9—N1	116.9 (3)	H7BB—C7B—H7BC	109.5
C11—C10—C9	117.3 (4)	C4—C8B—H8B1	109.5
C11—C10—C15	117.0 (4)	C4—C8B—H8B2	109.5
C9—C10—C15	125.7 (4)	H8B1—C8B—H8B2	109.5
C12—C11—C10	122.0 (4)	C4—C8B—H8B3	109.5
C12—C11—H11	119.0	H8B1—C8B—H8B3	109.5
C10—C11—H11	119.0	H8B2—C8B—H8B3	109.5
C11—C12—C13	119.3 (4)	C1T_1—O5T_1—C4T_1	105.8 (5)
C11—C12—H12	120.4	O5T_1—C1T_1—C2T_1	111.7 (6)
C13—C12—H12	120.4	O5T_1—C1T_1—H1TA_1	109.3
C12—C13—C14	121.9 (4)	C2T_1—C1T_1—H1TA_1	109.3
C12—C13—H13	119.1	O5T_1—C1T_1—H1TB_1	109.3
C14—C13—H13	119.1	C2T_1—C1T_1—H1TB_1	109.3
C13—C14—C9	117.9 (4)	H1TA_1—C1T_1—H1TB_1	108.0
C13—C14—C18	117.3 (3)	C1T_1—C2T_1—C3T_1	104.5 (6)
C9—C14—C18	124.7 (3)	C1T_1—C2T_1—H2TA_1	110.8
C10—C15—C16	110.8 (3)	C3T_1—C2T_1—H2TA_1	110.8
C10—C15—C17	110.9 (3)	C1T_1—C2T_1—H2TB_1	110.8
C16—C15—C17	108.9 (4)	C3T_1—C2T_1—H2TB_1	110.8
C10—C15—H15	108.7	H2TA_1—C2T_1—H2TB_1	108.9
C16—C15—H15	108.7	C2T_1—C3T_1—C4T_1	104.4 (6)
C17—C15—H15	108.7	C2T_1—C3T_1—H3TA_1	110.9
C15—C16—H16A	109.5	C4T_1—C3T_1—H3TA_1	110.9
C15—C16—H16B	109.5	C2T_1—C3T_1—H3TB_1	110.9
H16A—C16—H16B	109.5	C4T_1—C3T_1—H3TB_1	110.9
C15—C16—H16C	109.5	H3TA_1—C3T_1—H3TB_1	108.9
H16A—C16—H16C	109.5	O5T_1—C4T_1—C3T_1	107.0 (5)
H16B—C16—H16C	109.5	O5T_1—C4T_1—H4TA_1	110.3
C15—C17—H17A	109.5	C3T_1—C4T_1—H4TA_1	110.3
C15—C17—H17B	109.5	O5T_1—C4T_1—H4TB_1	110.3
H17A—C17—H17B	109.5	C3T_1—C4T_1—H4TB_1	110.3
C15—C17—H17C	109.5	H4TA_1—C4T_1—H4TB_1	108.6
H17A—C17—H17C	109.5		

Symmetry Code: (i) –x+1, -y+1, -z.

Table S7. Crystal data and structure refinement for Me_2-cAAC=O.

Compound	Me_2-cAAC=O
Empirical formula	$C_{20}H_{31}NO$
CCDC no.	927696
Molecular weight	301.46
Crystal size [mm]	0.16 × 0.14 × 0.10
Wavelength [pm]	1.54188
Crystal system	Monoclinic
Space group	$P2_1/n$
a [Å]	9.269(7)
b [Å]	17.342(10)
c [Å]	11.775(11)
α [°]	90.0
β [°]	96.71(4)
γ [°]	90.0
V [Å ^{3}]	1880(2)
Z	4
Temperature [K]	100(2)
ρ [Mgm^{-3}]	1.065
μ [mm^{-1}]	1.54188
F (000)	664
θ-area [°]	4.6 to 69.5
Total number reflect.	30611
Unique reflections	3254
R_{int}	0.0353
Number of restraints	0
Parameters	230
$R1$ [$I>2\sigma(I)$]	0.024
$wR2$ [$I>2\sigma(I)$]	0.021
$R1$ [all data]	0.027
$wR2$ [all data]	0.021
GooF	2.19
Extinction coefficient	
Largest diff. peak / hole max. / min. [10^3·e·nm^{-3}]	0.0198 and -0.127

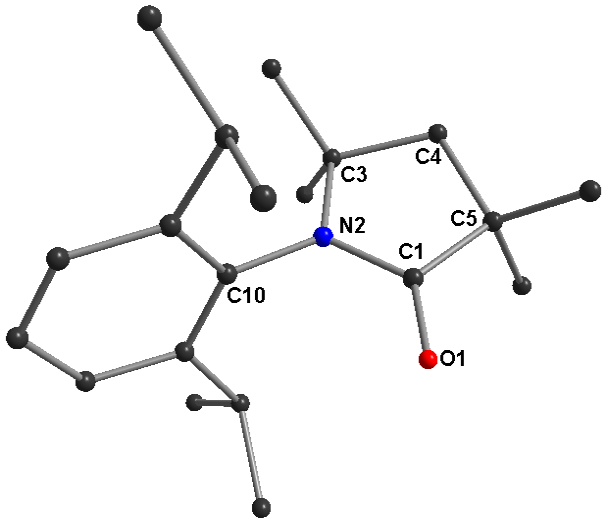

Figure S9. Crystal structure of Me_2-cAAC=O.

Table S8. Bond lengths [Å] and angles [°] for Me_2-cAAC=O.

O(1)—C(1)	1.2386 (10)	C(12)—C(13)	1.4059 (12)
N(2)—C(1)	1.3736 (10)	C(12)—H(12)	1.0823
N(2)—C(10)	1.4482 (10)	C(13)—C(14)	1.4058 (12)
C(4)—H(4A)	1.0937	C(13)—H(13)	1.0822
C(4)—H(4B)	1.0937	C(14)—C(15)	1.4118 (11)
C(6)—H(6A)	1.0914	C(14)—H(14)	1.0822
C(6)—H(6B)	1.0914	C(15)—C(19)	1.5367 (11)
C(6)—H(6C)	1.0914	C(16)—H(16)	1.0939
C(7)—H(7A)	1.0914	C(17)—H(17A)	1.0914
C(7)—H(7B)	1.0914	C(17)—H(17B)	1.0914
C(7)—H(7C)	1.0914	C(17)—H(17C)	1.0914
C(8)—H(8A)	1.0914	C(18)—H(18A)	1.0914
C(8)—H(8B)	1.0914	C(18)—H(18B)	1.0914
C(8)—H(8C)	1.0914	C(18)—H(18C)	1.0914
C(9)—H(9A)	1.0914	C(19)—H(19)	1.0939
C(9)—H(9B)	1.0914	C(20)—H(20A)	1.0914

C(9)—H(9C)	1.0914	C(20)—H(20B)	1.0914
C(10)—C(11)	1.4292 (11)	C(20)—H(20C)	1.0914
C(10)—C(15)	1.4270 (11)	C(21)—H(21A)	1.0914
C(11)—C(12)	1.4123 (11)	C(21)—H(21B)	1.0914
C(11)—C(16)	1.5363 (12)	C(21)—H(21C)	1.0914
C(1)—N(2)—C(10)	122.73 (6)	C(12)—C(11)—C(16)	119.15 (7)
O(1)—C(1)—N(2)	125.44 (7)	C(11)—C(12)—C(13)	121.08 (8)
N(2)—C(10)—C(11)	118.98 (7)	C(12)—C(13)—C(14)	119.70 (8)
N(2)—C(10)—C(15)	120.07 (7)	C(13)—C(14)—C(15)	121.33 (8)
C(11)—C(10)—C(15)	120.95 (7)	C(10)—C(15)—C(14)	118.20 (7)
C(10)—C(11)—C(12)	118.37 (8)	C(10)—C(15)—C(19)	122.81 (7)
C(10)—C(11)—C(16)	122.30 (7)	C(14)—C(15)—C(19)	118.79 (7)

(S4) Solid state NMR

All the solid-state experiments on compound **2** were done at a field strength of 9.4 T (400 MHz) using an Avance spectrometer (Bruker Biospin, Germany) at room temperature. ^{29}Si CP MAS NMR spectra were acquired using a 2.5 mm triple channel probe whereas ^{13}C CPMAS NMR spectra were acquired with a 4 mm triple channel probe. The carbon spectra were calibrated by referencing externally to the ^{13}CH resonance (31.46 ppm) of solid adamantane. Similarly, ^{29}Si spectra were externally referenced to the single silicon resonance (0 ppm) of sodium salt of trimethyl-slilyl-propanoic acid. For silicon, the spectra were acquired at two spinning speeds of 7 and 18 kHz to determine the isotropic chemical shifts as shown in Figure SB for compound **2**. In a similar fashion, the carbon spectra were recorded at 8 kHz and 11 kHz MAS. Since, the compounds are air-sensitive; the samples were filled into the rotors in a glove box.

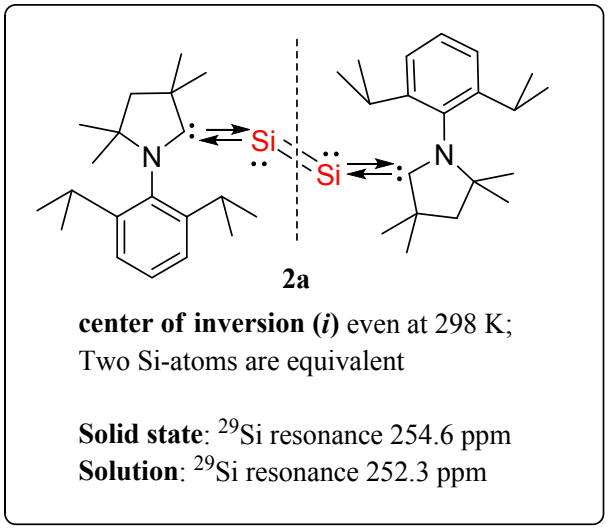

2a

center of inversion (*i*) even at 298 K;
Two Si-atoms are equivalent

Solid state: ^{29}Si resonance 254.6 ppm
Solution: ^{29}Si resonance 252.3 ppm

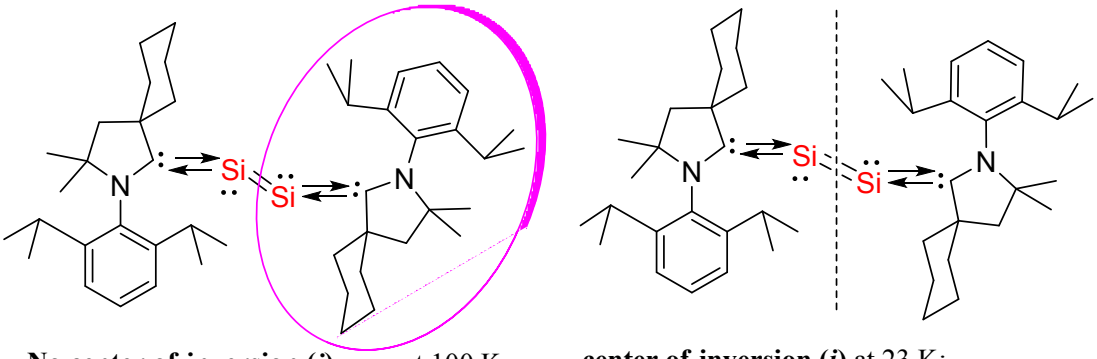

No center of inversion (*i*) even at 100 K;
Two Si-atoms are not equivalent

center of inversion (*i*) at 23 K;
Both Si-atoms are equivalent

2b

Solid state: ^{29}Si resonances 190.1 and 318.3 ppm
Solution: ^{29}Si resonance 249.1 ppm

Scheme S6: In $(Me_2\text{-cAAC})_2Si_2$ (**2a**) (top) center of inversion is always present while in $(Cy\text{-cAAC})_2Si_2$ (**2b**) (bottom) the presence of center of inversion is dependent on temperature. It is concluded from temperature dependent X-ray single crystal diffractions and solid state NMR. Structural comparison between **2a** and **2b** clearly shows that the carbene moieties (at 100 K) are evenly disordered in **2a** but not in **2b** (Figures S5-S8). This is also clearly observed in solid state ^{13}C and ^{29}Si NMR (see below).

The ^{29}Si NMR spectra of $(Me_2\text{-cAAC})_2Si_2$ (**2a**) and $(Cy\text{-cAAC})_2Si_2$ (**2b**) which are recorded in C_6D_6 show single resonances at δ = 252.6 ppm for **2a** and 249.1 ppm for **2b** , they are more downfield shifted than that of $(NHC)_{2Si}$ (δ = 224.5 ppm).[S10] The ^{29}Si resonance at 249.1 ppm (**4**) in solution falls in between 190.2 and 318.3 ppm. The ^{13}C NMR spectra of **2a** and **2b** exhibit a resonance at δ = 236.7 ppm for **2a** and 234.7 ppm for **2b** which are more upfield shifted than that of cAAC: (δ = 304.2 ppm for Me_2-cAAC: and 309.4 ppm for Cy-cAAC:)[S1] but more downfield than that of $(Me_2\text{-cAAC})_2Si$ (δ = 210.0 ppm).[S11] The NMR spectra of both the compounds in solution

suggest that two silicon atoms are equivalent in solution while in solid state they are not. Robinson et al. have proposed [S12a] that NHC: stabilized P_2 allotrope can have two canonical forms; NHC:→P-P←:NHC and NHC=P-P=NHC. The former conformer [S12a] was established as the predominating product based on the chemical shift values of ^{31}P NMR while the latter one [S12b] was shown to be the only conformer cAAC=P-P=CAAc for the cAAC: analogue.

Solid-state CPMAS NMR experiments: All the solid-state experiments were done at either a field strength of 9.4 T (^1H, 400 MHz) or 14.1 T (^1H, 600 MHz) using Avance III HD spectrometer (Bruker Biospin, Germany). ^{29}Si- and ^{13}C CPMAS NMR spectra were acquired using either a 2.5 mm or a 4 mm triple channel probe. The carbon spectra were calibrated by referencing externally to the ^{13}CH resonance (31.46 ppm) of solid adamantane. Similarly, ^{29}Si spectra were externally referenced to the single silicon resonance (0 ppm) of sodium salt of trimethyl-slilyl-propanoic acid. For both nuclei, the spectra were acquired at two spinning speeds to determine the isotropic chemical shifts. Since, the compounds are air-sensitive the samples were filled into the rotors in a glove box.

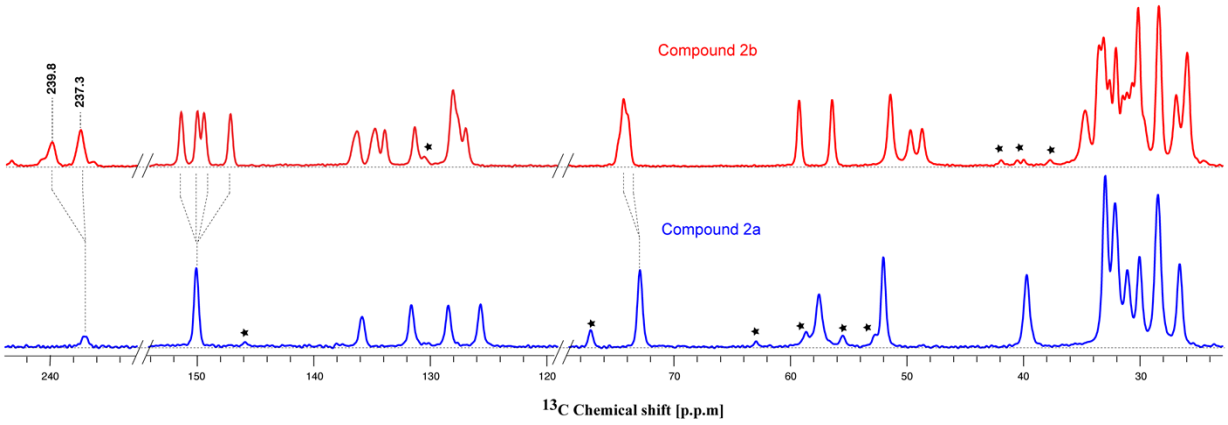

Figure S10. A comparison of solid-state ^{13}C CP MAS spectra of compound **2a** and **2b** at a spinning speed of 11 kHz. The spinning sideband regions are denoted by ``*´´ symbol. The carbene resonances are indicated in the figure. (T = 298 K)

Compound 2a: ^{13}C (solid state NMR 298 K, δ ppm): 237.1 (C), 150.1, 135.8, 131.6, 128.4, 125.6, 72.9, 57,5, 52.0, 39.7, 32.1, 31.1, 30.1, 28.5, 26.6.

Compound 2b: ^{13}C (solid state NMR 298 K, δ ppm): 239.8 (C), 237.3, 151.3, 149.9, 149.4, 147.1, 136.3, 134.7, 133.9, 131.3, 128.0, 127.6, 127.0, 74.3, 73.9, 59.2, 56.4, 51.4, 49.7, 48.6, 34.7, 33.5, 33.1, 32.6, 32.0, 31.5, 31.1, 30.7, 30.1, 29.6, 23.9, 26.9, 25.9.

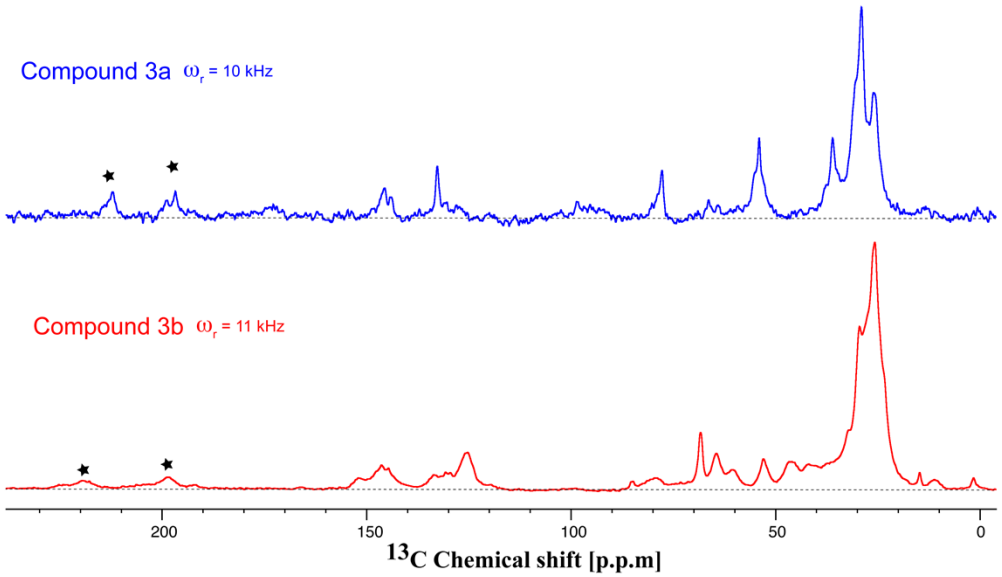

Figure S11. A comparison of solid-state ^{13}C CP MAS spectra of compound **3a** and **3b.** The spinning sideband regions are denoted by "★" symbol. The peaks are broader in comparison with the compound **2a** and **2b**. (T = 298 K)

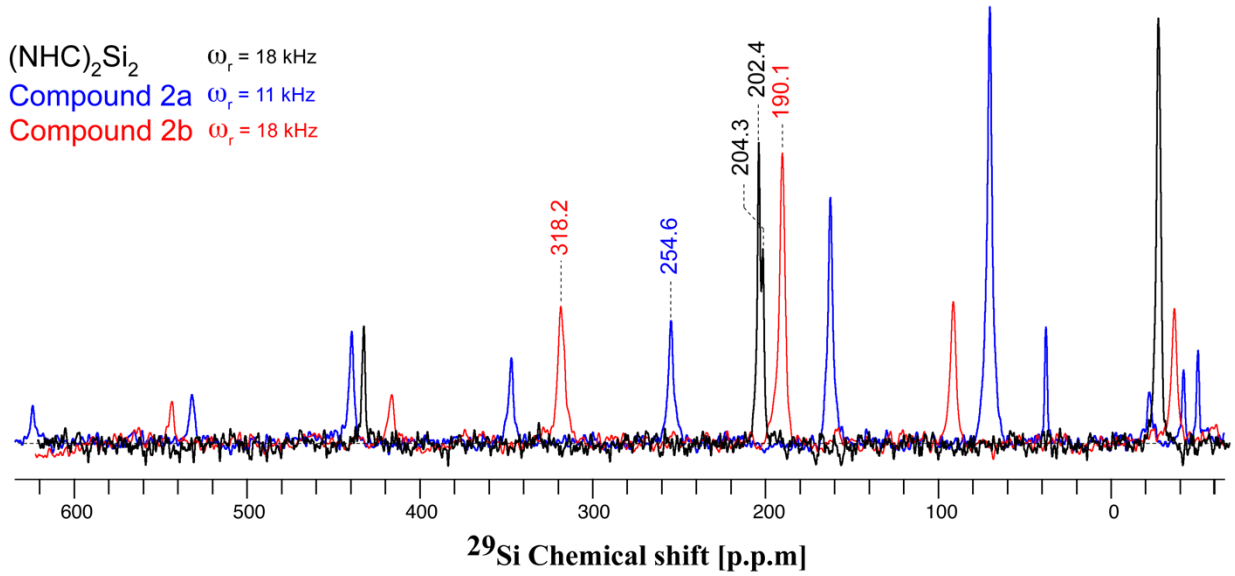

Figure S12. Comparison of Solid-state ^{29}Si CP MAS spectra of $(NHC)_2Si_2$, compound **2a**, and compound **2b.** Isotropic chemical shift values are indicated in the figure. All other peaks are spinning sidebands.

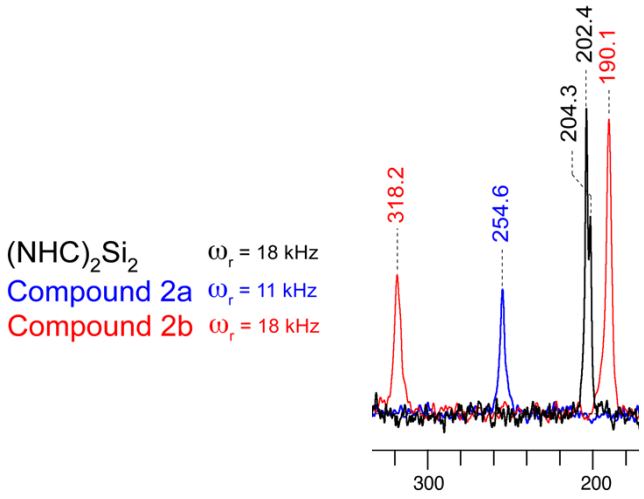

Figure S13. Solid state ^{29}Si CPMAS NMR spectra of $(Me_2\text{-cAAC})_2Si_2$ (**2a**) (blue), $(Cy\text{-cAAC})_2Si_2$ (**2b**) (red) and $(NHC)_2Si_2$ (black).

(S5) Theoretical calculations

Computational Details:

All calculations were performed in Gaussian09 quantum package.[S13] Intermediates are optimized using the global-hybrid meta-GGA to DFT functional, R-M06-2X[S14] with SVP[S15] basis sets for all atoms. Geometries were fully optimized without symmetry constraints. Harmonic force constants were computed at the optimized geometries to confirm if they were located at minima or saddle point on the potential energy surface. For further validation of the energy change, we have also performed single point calculation of optimized geometry incorporating higher basis set TZVP[S16] for all atoms. Solvation energies in THF (ε = 7.426) were evaluated by a self-consistent reaction field (SCRF) approach using the SMD continuum solvation model.[S17] NBO analysis were performed at R-M06-2X/TZVP//R-M06-2X/SVP level of theory. All the energy values reported in the manuscript are at R-M06-2X/TZVP/SMD//R-M06-2X/SVP level. The wavefunction file generated from the quantum code, were used to perform QTAIM[S18] analysis in the AIMALL program suite. We have applied Bader's AIM (Atoms-in-molecule)[S19] concept to characterize the electron distribution in **3a**. Any bonded pair of atoms has a bond path, *i.e;* a connecting line with maximum electron density. The bond critical point (BCP) is a point on this line where the gradient $\nabla\rho(r)$ of the density is equal to zero. The magnitude of the electron density, $\rho(r)$ and its Laplacian, $\nabla^2\rho(r)$ at the BCP provide information about the strength and type of bond.

The Laplacian indicates whether the density is locally concentrated ($\nabla^2\rho<0$) or depleted ($\nabla^2\rho>0$). Optimized geometries and orbital diagrams are rendered in the Chemcraft visualization software.[S20]

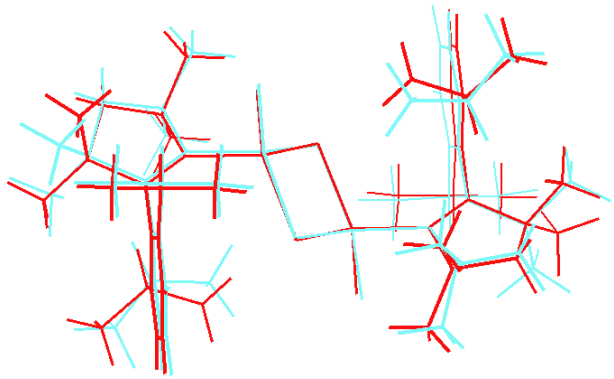

Figure S14. Superposition of crystal structure of **3a** with the optimized geometry at R-M06-2X/SVP level of theory.

Table S9. Topological parameters of important (3,-1) bond critical points (BCPs) of **3a**.

Bond	ρ (e/Å^3)	$\nabla^2\rho$ (e/Å^5)	DI
N1-C1	0.343	-0.648	1.34
C1-Si1	0.095	+0.051	0.43
Si1-Se1	0.083	+0.009	0.58
Si1-Se1´	0.083	+0.005	0.60
Si1-Se2	0.104	+0.051	0.86

Table S10. Details Electronic Spectrum for the DFT optimized species **3a** at R-B3LYP/TZVP//R-M06-2X/SVP level. The cut-off on oscillator strength: 0.02. Total no. of states in the calculation: 20.

λ (nm)[1]	f[2]	ΔE (cm^{-1})[3]	Orbitals (percentage contribution)[4]
441	0.030	22660.3.	H-1→L(73%); H-3→L(17%)
430	0.029	23249.9	H-1→L+1(86%); H-3→L+1(5%);
418	0.028	23892.7	H-2→L(73%); H-3→LUMO(12%)
409	0.062	24421.8	H-2→L+1(90%); H-2→L(6%)

[1] Wavelength of the transition. [2] The oscillator strength of the transition. [3] Excitation energies for each transition. [4] Molecular orbitals involved in the transitions; H = HOMO, L = LUMO. The respective contributions are in parentheses.

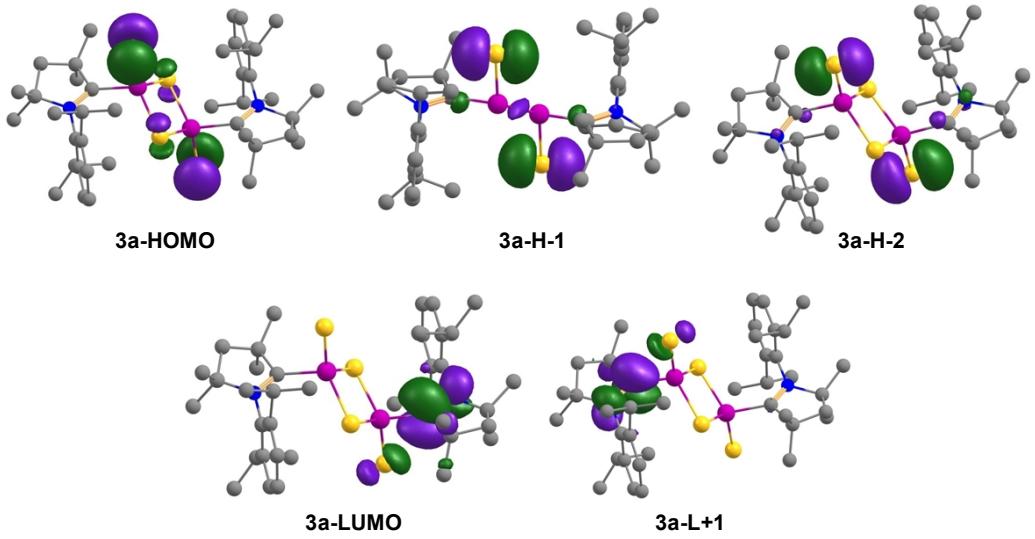

Figure S15. KS-MOs of some intermediates (isosurface = 0.05 au) and compound **3a**. Hydrogen atoms are omitted for clarity. H and L designate HOMO and LUMO.

Table S11. Calculated chemical shifts values (in ppm) of selected atoms for **3a** at R-B3LYP/TZVP//R-M06-2X/SVP level of theory.

C1	C1´	Si1	Si1´	Se1	Se1´	Se2	Se2´
209.4	207.5	12.4	18.2	-536.8	-526.6	-637.9	-600.6

Table S12. Cartesian coordinates (in Å) of the optimized structures of reactant, intermediates and product at R-M06-2X/SVP level of theory. Energy terms are in kcal/mol.

2a

Energy: -1410525.3847169

Si	0.11003	0.94383	0.59695
N	-0.96236	3.33769	-0.48777
C	-2.69571	1.79606	-0.32318
C	-2.17599	4.17078	-0.76854
C	0.98271	4.49002	0.50947
C	1.05019	3.76119	-1.83949

C	0.36762	3.87700	-0.60691
C	0.52008	2.97091	-3.02716
C	2.31337	4.34967	-1.95605
C	-1.19389	2.05281	-0.17280
C	0.38026	4.51037	1.90783
C	-2.16905	5.46631	0.03812
C	0.45589	3.80760	-4.30962
C	2.24776	5.06113	0.33573
C	-2.27297	4.54454	-2.24987
C	-3.29556	0.93587	0.79026
C	2.90469	5.01023	-0.88682
C	-3.28710	3.22021	-0.30227
C	0.18520	5.93762	2.43604
C	-2.93867	1.09579	-1.67163
C	1.26246	3.72923	2.89154
C	1.38004	1.72331	-3.26325
H	-0.49119	2.62332	-2.78186
H	2.84792	4.27407	-2.90511
H	-0.59311	3.99986	1.86495
H	-1.30797	6.09522	-0.23237
H	-2.14429	5.27095	1.11710
H	-3.08694	6.02928	-0.18567
H	-0.02207	3.22949	-5.11435
H	1.46659	4.07358	-4.65449
H	-0.10688	4.74146	-4.17699
H	2.73211	5.54344	1.18727
H	-3.16331	5.17059	-2.40467
H	-2.35409	3.66935	-2.90541
H	-1.39141	5.12858	-2.54958
H	-3.05028	1.34308	1.78264
H	-2.90965	-0.09118	0.73656
H	-4.39147	0.90736	0.68045
H	3.88968	5.46610	-1.00016
H	-3.56618	3.47472	0.73218
H	-4.19055	3.30607	-0.92393
H	-0.39075	6.57079	1.74951
H	1.15901	6.42403	2.59975

H	-0.33648	5.91482	3.40467
H	-4.02138	0.97635	-1.83157
H	-2.47511	0.09829	-1.67516
H	-2.52534	1.66294	-2.51686
H	1.43295	2.70348	2.53917
H	0.77449	3.68055	3.87667
H	2.23615	4.22644	3.02223
H	0.96178	1.12284	-4.08520
H	1.40859	1.09446	-2.36367
H	2.41023	2.00305	-3.53490
Si	-0.11003	-0.94383	-0.59695
N	0.96236	-3.33769	0.48777
C	2.69571	-1.79606	0.32318
C	2.17599	-4.17078	0.76854
C	-0.98271	-4.49002	-0.50947
C	-1.05019	-3.76119	1.83949
C	-0.36762	-3.87700	0.60691
C	-0.52008	-2.97091	3.02716
C	-2.31337	-4.34967	1.95605
C	1.19389	-2.05281	0.17280
C	-0.38026	-4.51037	-1.90783
C	2.16905	-5.46631	-0.03812
C	-0.45589	-3.80760	4.30962
C	-2.24776	-5.06113	-0.33573
C	2.27297	-4.54454	2.24987
C	3.29556	-0.93587	-0.79026
C	-2.90469	-5.01023	0.88682
C	3.28710	-3.22021	0.30227
C	-0.18520	-5.93762	-2.43604
C	2.93867	-1.09579	1.67163
C	-1.26246	-3.72923	-2.89154
C	-1.38004	-1.72331	3.26325
H	0.49119	-2.62332	2.78186
H	-2.84792	-4.27407	2.90511
H	0.59311	-3.99986	-1.86495
H	1.30797	-6.09522	0.23237
H	2.14429	-5.27095	-1.11710

H	3.08694	-6.02928	0.18567
H	0.02207	-3.22949	5.11435
H	-1.46659	-4.07358	4.65449
H	0.10688	-4.74146	4.17699
H	-2.73211	-5.54344	-1.18727
H	3.16331	-5.17059	2.40467
H	2.35409	-3.66935	2.90541
H	1.39141	-5.12858	2.54958
H	3.05028	-1.34308	-1.78264
H	2.90965	0.09118	-0.73656
H	4.39147	-0.90736	-0.68045
H	-3.88968	-5.46610	1.00016
H	3.56618	-3.47472	-0.73218
H	4.19055	-3.30607	0.92393
H	0.39075	-6.57079	-1.74951
H	-1.15901	-6.42403	-2.59975
H	0.33648	-5.91482	-3.40467
H	4.02138	-0.97635	1.83157
H	2.47511	-0.09829	1.67516
H	2.52534	-1.66294	2.51686
H	-1.43295	-2.70348	-2.53917
H	-0.77449	-3.68055	-3.87667
H	-2.23615	-4.22644	-3.02223
H	-0.96178	-1.12284	4.08520
H	-1.40859	-1.09446	2.36367
H	-2.41023	-2.00305	3.53490

3a

Energy: -7438051.2239691

Se	5.56251	4.79948	-0.09400
Si	7.16914	4.82230	1.57781
N	5.95909	6.98182	3.14908
C	7.04788	6.37835	2.74283
Se	7.19337	3.34178	3.14464
C	8.25034	6.92197	3.51531
C	4.68733	6.95840	2.43841
C	4.50238	7.92855	1.42626

C	3.69983	5.99402	2.72937
C	5.57411	8.92954	1.02121
H	6.26822	9.02612	1.85728
C	3.84947	4.84358	3.71617
H	4.87022	4.85999	4.12207
C	3.29625	7.92678	0.72479
H	3.14410	8.65523	-0.07195
C	2.50480	6.05525	2.00069
H	1.72821	5.31722	2.20732
C	2.29794	7.00417	1.01146
H	1.36183	7.01741	0.45146
C	2.83288	4.92457	4.86299
H	1.80767	4.81322	4.47817
H	2.87772	5.87096	5.41544
H	3.00862	4.10376	5.57379
C	5.00451	10.32508	0.75267
H	5.82670	11.04731	0.64524
H	4.34791	10.66497	1.56761
H	4.42822	10.35430	-0.18352
C	6.12648	7.79952	4.42101
C	3.67761	3.49261	3.00667
H	2.63486	3.34998	2.68274
H	3.93876	2.67828	3.69769
H	4.33530	3.39964	2.13378
C	6.38760	8.43056	-0.17564
H	5.74243	8.15376	-1.02266
H	6.98066	7.54068	0.07931
H	7.08806	9.20855	-0.51571
C	9.37305	5.94377	3.85973
H	9.83069	5.51330	2.95759
H	9.01052	5.11454	4.47704
H	10.15248	6.49913	4.40409
C	8.85018	8.04528	2.63872
H	9.25023	7.63201	1.70211
H	9.67310	8.51867	3.19402
H	8.11951	8.82166	2.38074
Se	8.99646	5.11979	0.18306

Si	7.39437	5.00722	-1.49193
N	8.74597	2.96497	-3.04402
C	7.59782	3.42063	-2.61077
Se	7.34504	6.40545	-3.13503
C	6.44694	2.71359	-3.33944
C	9.99120	3.02797	-2.30282
C	10.17151	2.02089	-1.32939
C	10.95378	4.02455	-2.53366
C	9.12582	0.95335	-1.03780
H	8.46589	0.87216	-1.91344
C	10.81092	5.12648	-3.56770
H	9.79740	5.07449	-3.98705
C	11.34050	2.04934	-0.56898
H	11.49246	1.29667	0.20529
C	12.11212	3.99784	-1.74674
H	12.86969	4.76817	-1.90037
C	12.30510	3.03053	-0.77138
H	13.21001	3.04054	-0.16212
C	11.84167	4.94781	-4.69007
H	12.86023	5.12446	-4.31141
H	11.82617	3.93306	-5.11466
H	11.65524	5.66749	-5.50104
C	9.74636	-0.42923	-0.81846
H	8.95409	-1.18998	-0.76965
H	10.44017	-0.69948	-1.62866
H	10.29819	-0.47795	0.13131
C	8.63919	2.22767	-4.36322
C	10.95246	6.51677	-2.93945
H	11.97509	6.68566	-2.56768
H	10.73029	7.28716	-3.69222
H	10.24451	6.65470	-2.11135
C	8.25960	1.35788	0.15925
H	8.87568	1.56151	1.04781
H	7.68397	2.27401	-0.03814
H	7.54396	0.56041	0.41197
C	5.47681	3.63639	-4.08508
H	5.00136	4.34937	-3.39797

H	5.98128	4.22490	-4.86135

(S6) Raman spectra of 3a

Raman spectra are recorded on solid sample of **3a** which exhibit Raman bands at 1490.9 cm^{-1} with a shoulder at 1475.9 cm^{-1}. The calculated Raman bands with the highest intensities are observed at 1605.7 and 1595.8 cm^{-1}. The two bands of which the later one is shouldered with the highest intensity at 1605.7 cm^{-1}. The Raman bands are observed in the range of 400 to 50 cm^{-1} (strong lines are at around 240 cm^{-1}) for different polymorphs of $(SiSe_2)_n$.[S21]

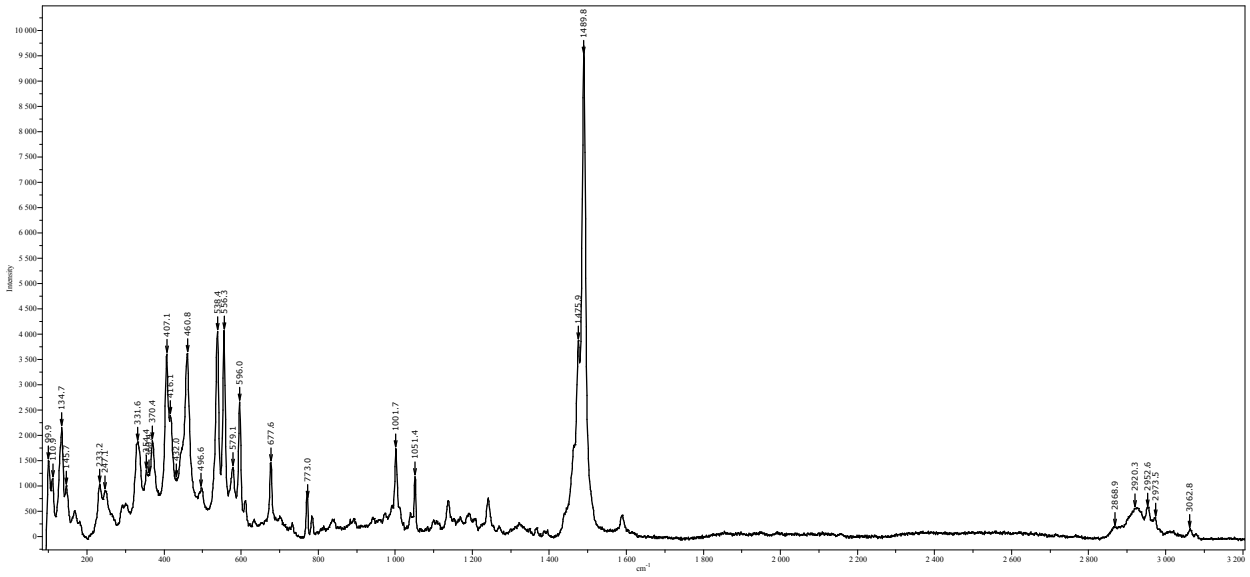

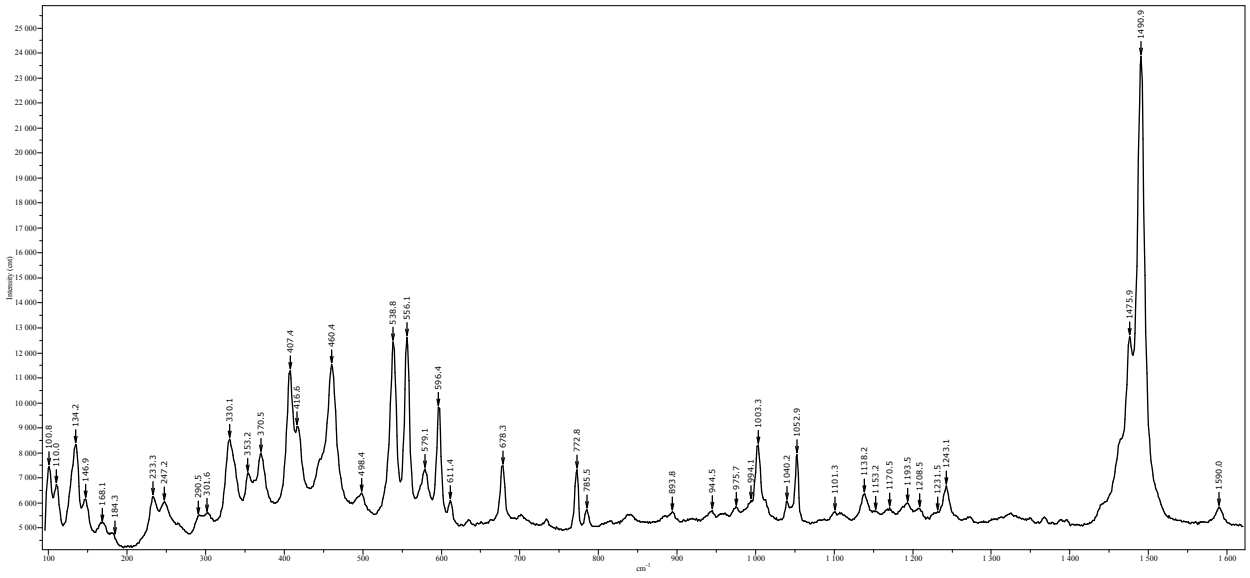
Intensity (cps)
cm-1
100.8
110.0
134.2
146.9
168.1
184.3
233.3
247.2
290.5
301.6
330.1
353.2
370.5
407.4
416.6
460.4
498.4
538.8
556.1
579.1
596.4
611.4
678.3
772.8
785.5
893.8
944.5
975.7
994.1
1003.3
1040.2
1052.9
1101.3
1138.2
1153.2
1176.5
1193.5
1208.5
1231.5
1243.1
1475.9
1490.9
1590.0

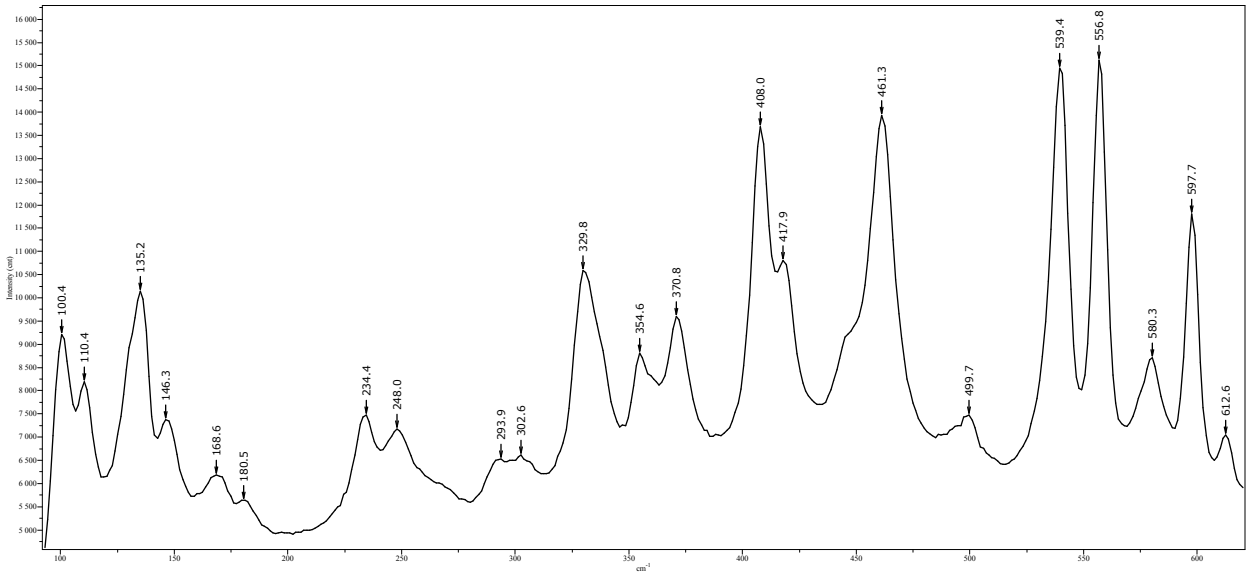

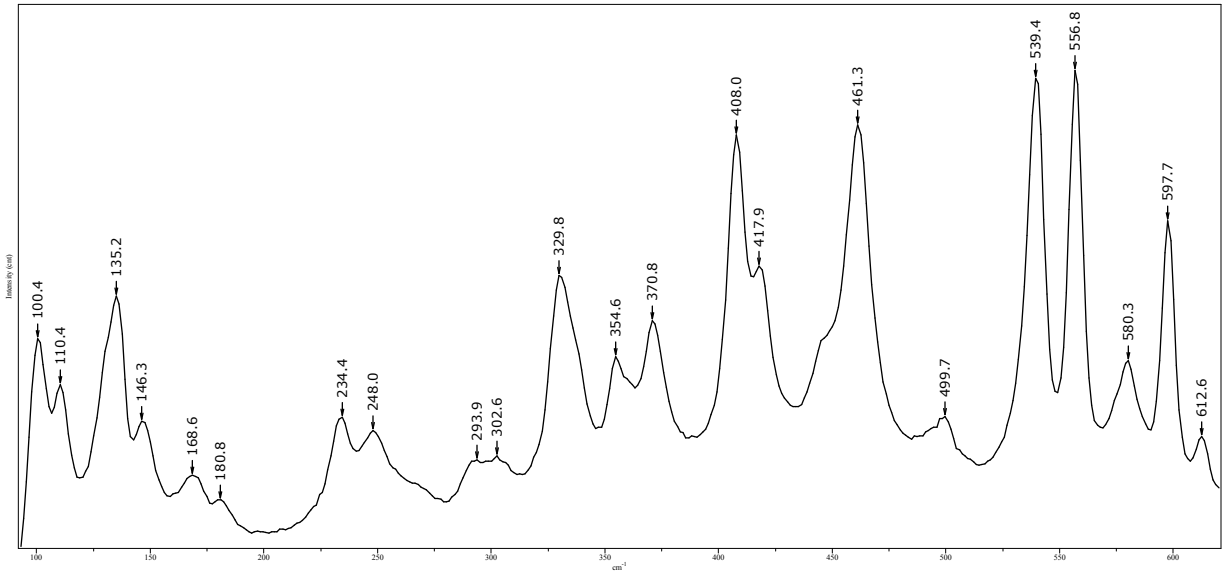

(S7) NMR spectra

[1]H NMR spectrum of Compound 2a.

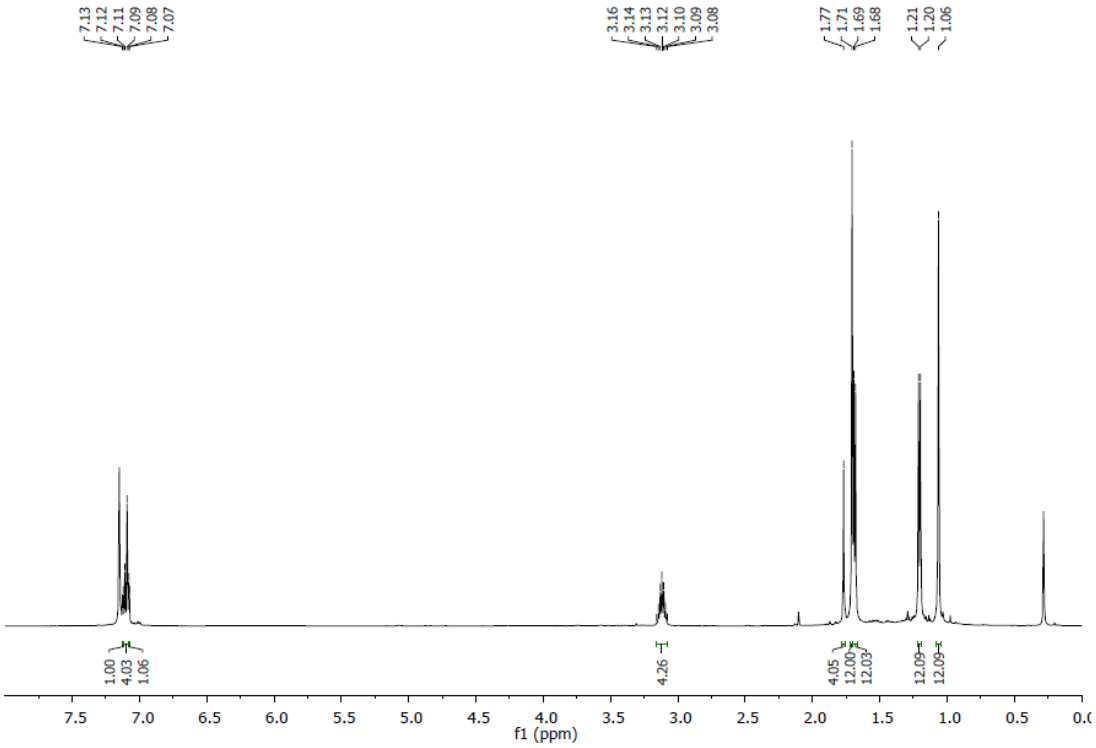

[13]C NMR spectrum of Compound 2a.

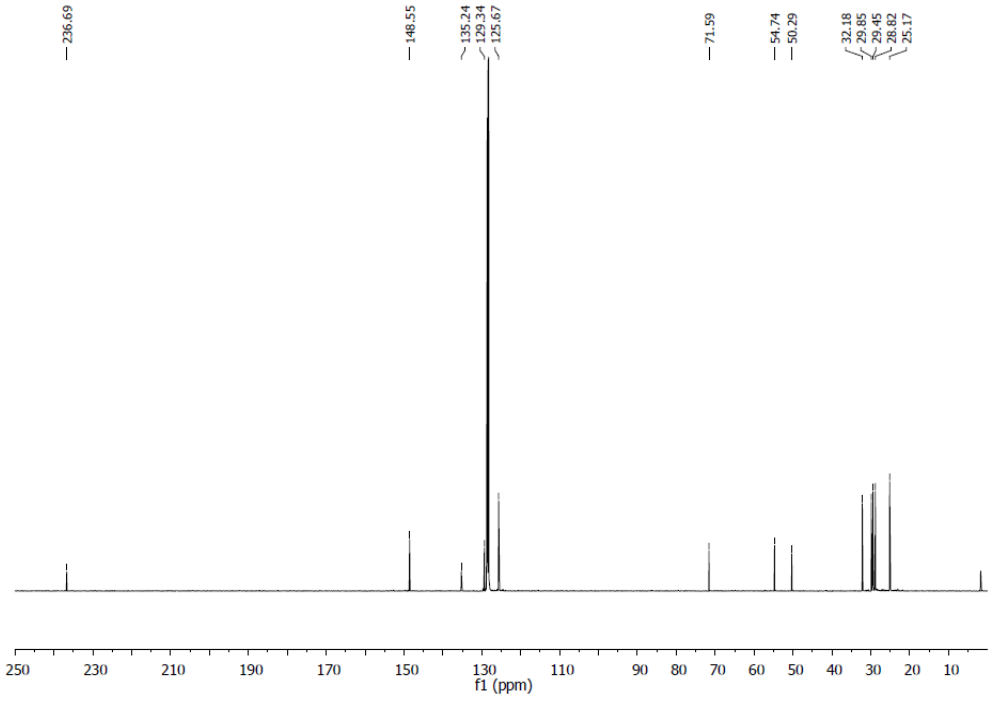

^{29}Si NMR spectrum of Compound 2a.

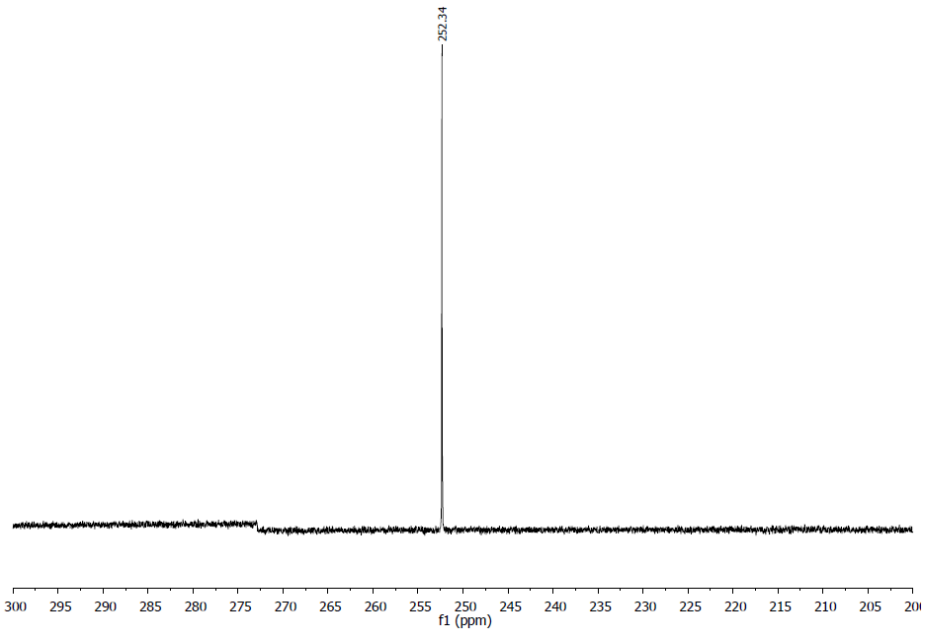

^{1}H NMR spectrum of Compound 2b.

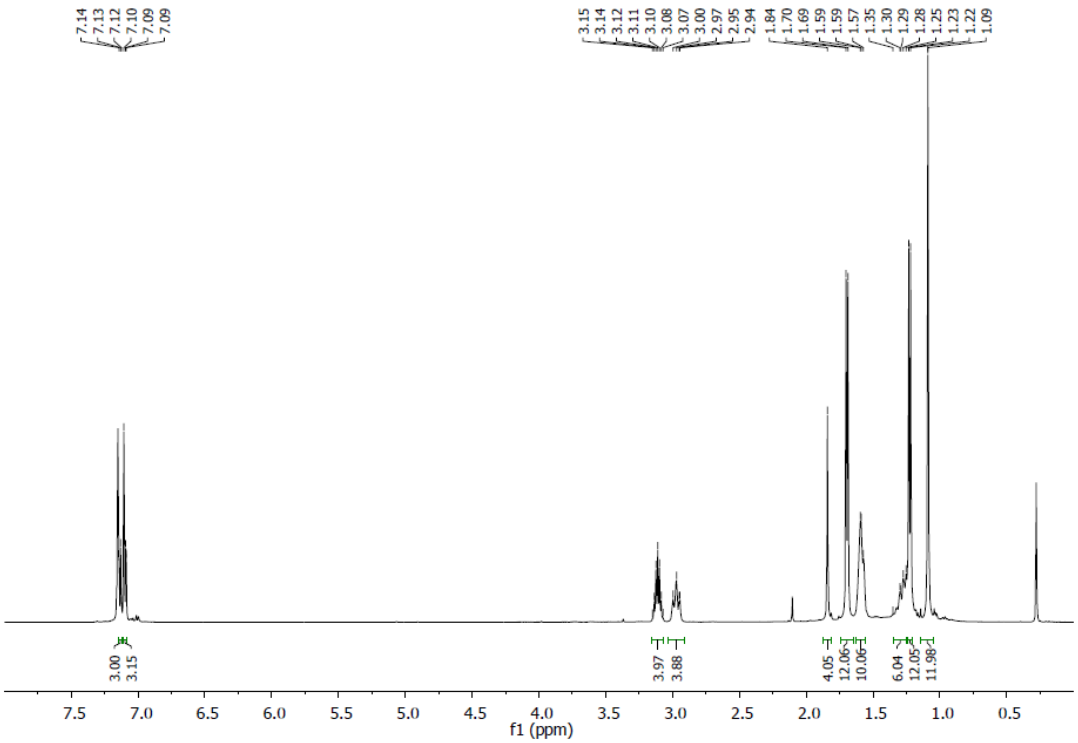

^{13}C NMR spectrum of Compound 2b.

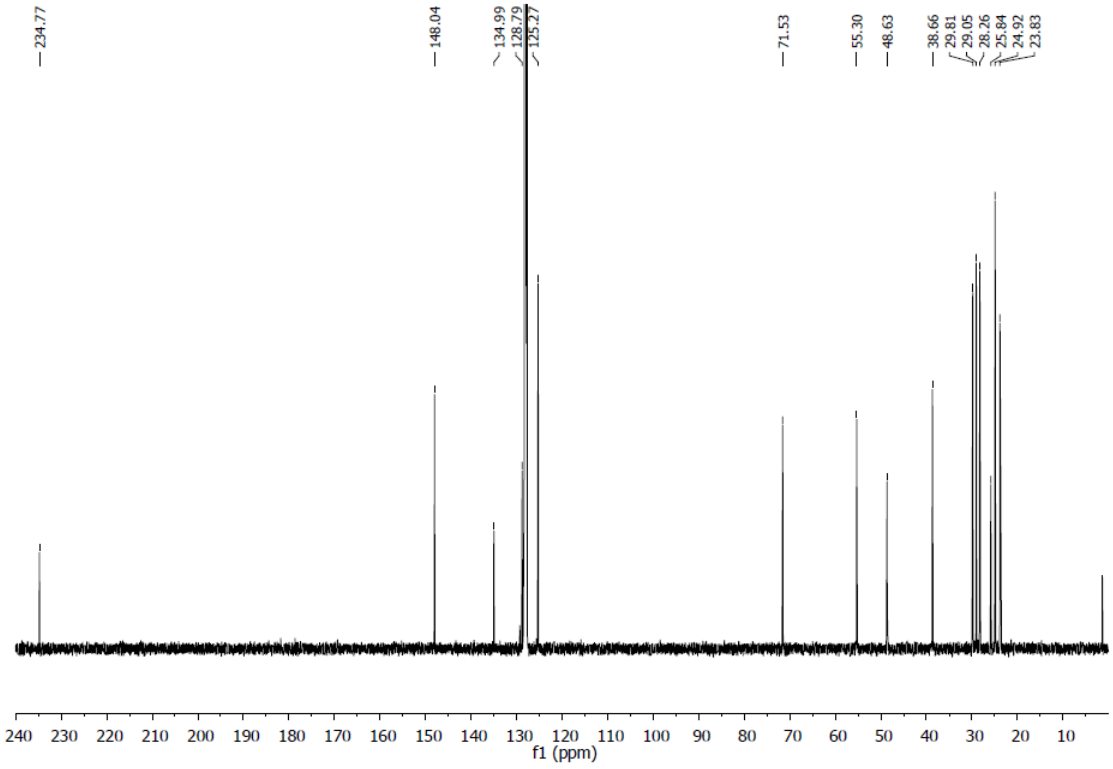

^{29}Si NMR spectrum of Compound 2b.

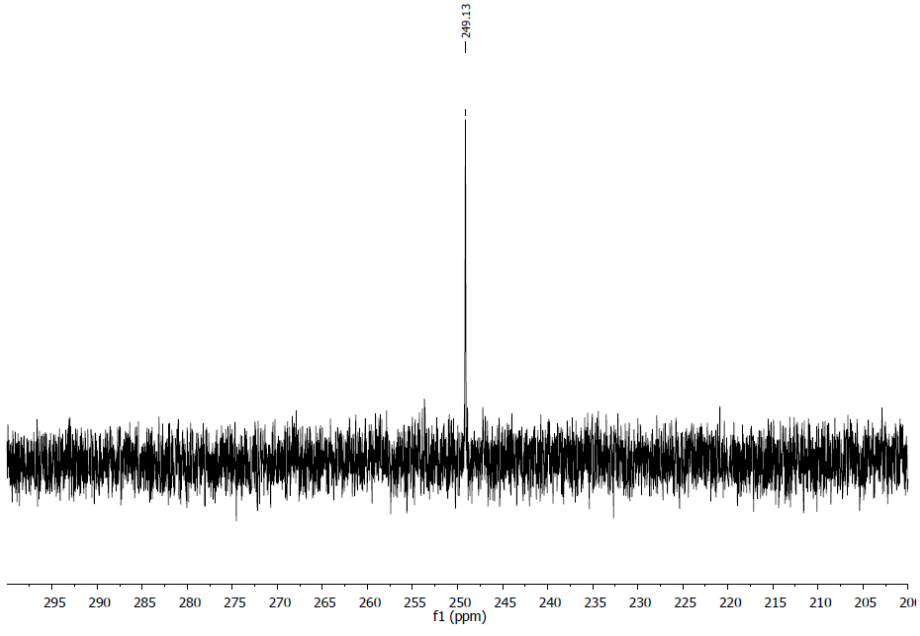

(S8) EI-mass spectra of 3a

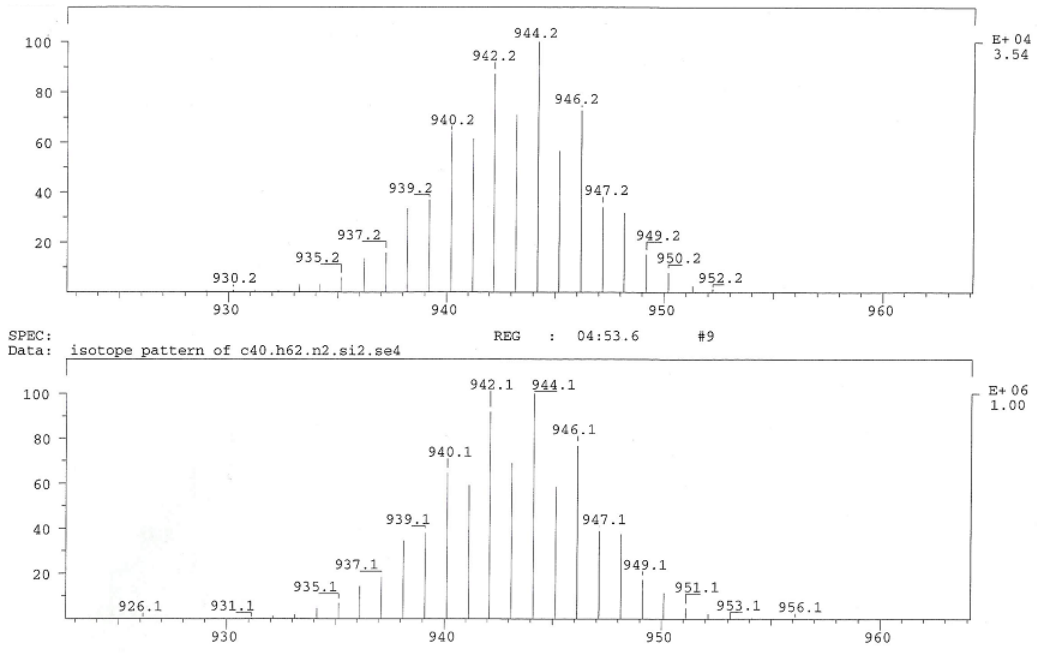

Experimental (top) and simulated (bottom) EI-MS mass spectra of **3a**: (*m/Z*(100%); 944.2).

When **3a** is heated to 300 °C it decomposes to Me_2-cAAC=Se which is characterized by mass spectrum (below)

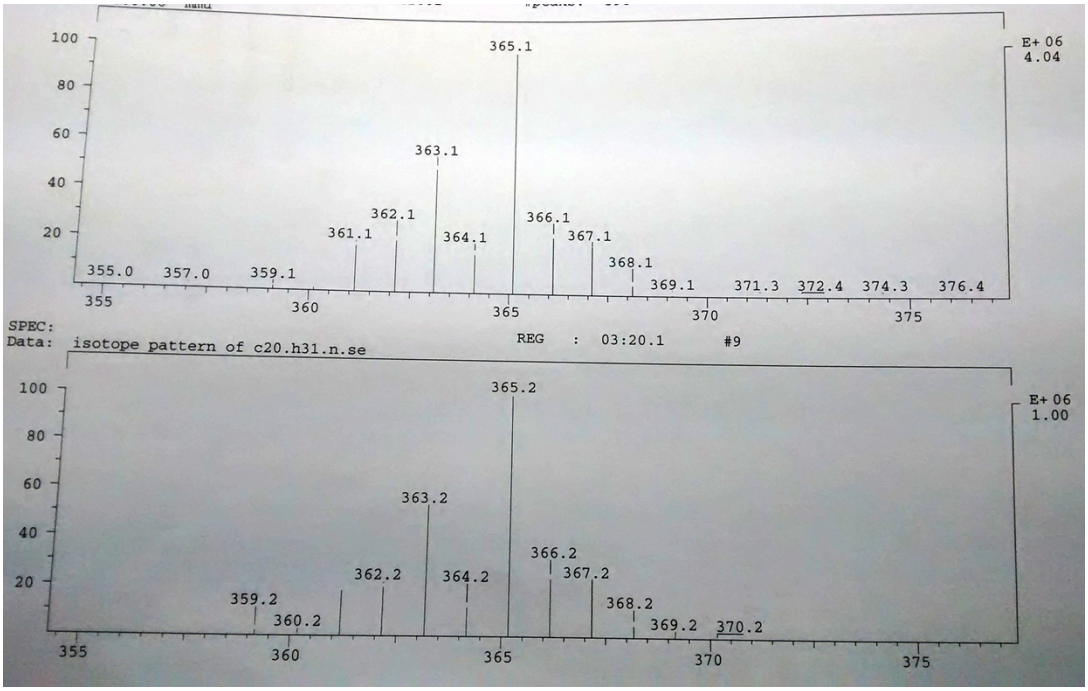

Experimental (top) and simulated (bottom) EI-MS mass spectra of Me_2-cAAC=Se: (*m/Z*(100%); 365.1).

(S9) References

(S1) V. Lavallo, Y. Canac, C. Präsang, B. Donnadieu, G. Bertrand, *Angew. Chem. Int. Ed*., 2005, *44*, 5705; *Angew. Chem.* 2005, **117**, 5851.

(S2) K. C. Mondal, H. W. Roesky, A. C. Stückl, F. Ihret, W. Kaim, B. Dittrich, B. Maity, D. Koley, *Angew. Chem. Int. Ed*., 2013, **52**, 11804; *Angew.Chem*., 2013, **125**, 12020.

(S3) K. C. Mondal, P. P. Samuel, H. W. Roesky, R. R. Aysin, L. A. Leites, S. Neudeck, J. Lübben, B. Dittrich, M. Hermann, G. Frenking. *J. Am. Chem. Soc*., 2014, **136**, 8919.

(S4) Tretiakov, M.; Shermolovich, Y. G.; Singh, A. P.; Samuel, P. P.; Roesky, H. W.; Niepötter, B.; Visscher, A.; Stalke, D. *Dalton Trans*., 2013, **42**, 12940.

(S5) K. C. Mondal, P. P. Samuel, M. Tretiakov, A. P. Singh, H. W. Roesky, A. C. Stückl, B. Niepötter, E. Carl, H. Wolf, R. Herbst-Irmer, D. Stalke, *Inorg. Chem*., 2013, **52**, 4736.

(S6) G. M. Sheldrick, SADABS 2008/2, Göttingen, 2008.

(S7) G. M. Sheldrick, *Acta Cryst*., 2008, **A64**, 112.

(S8) B. Dittrich, C. B. Hübschle, K. Pröpper, F. Dietrich, T. Stolper, J. Holstein, *J. Acta Cryst*., 2013, **B69**, 91.

(S9) Volkov, A.; Macchi, P.; Farrugia, L. J.; Gatti, C.; Mallinson, P.; Richter, T.; Koritsanszky, T. XD2006 -A Computer Program Package for Multipole Refinement, Topological Analysis of Charge Densities and Evaluation of Intermolecular Energies from Experimental or Theoretical Structure Factors. University at Buffalo, NY, USA; University of Milano, Italy; University of Glasgow, UK; CNRISTM, Milano, Italy; Middle Tennessee State University, TN, USA; University of Berlin, Berlin, Germany.

(S10) Y. Wang, Y. Xie, P. Wei, R. B. King, H. F. Schaefer III, P. v. R. Schleyer, G. H. Robinson, *Science,* 2008, **321**, 1069.

(S11) K. C. Mondal, H. W. Roesky, M. C. Schwarzer, G. Frenking, B. Niepötter, H. Wolf, R. Herbst-Irmer, D. Stalke, *Angew. Chem. Int. Ed*., 2013, **52**, 2963; *Angew.Chem*., 2013, **125**, 3036.

(S12) (*a*) Y. Wang, Y. Xie, P. Wie, R. B. King, H. F. Schaefer, III, P. v. R. Schleyer, G. H. Robinson, *J. Am. Chem. Soc.,* 2008, **130**,14970; (*b*) O. Back, G. Kuchenbeiser, B. Donnadieu, G. Bertrand, *Angew. Chem. Int*. Ed., 2009, **48**, 5530; *Angew. Chem*., 2009, **121**, 5638.

(S13) Gaussian 09, Revision C.01, M. J. Frisch et al. Gaussian, Inc., Wallingford CT, 2009. Full reference for Gaussian09: Gaussian 09, Revision **C.01**, M. J. Frisch, G. W. Trucks, H. B. Schlegel, G. E. Scuseria, M. A. Robb, J. R. Cheeseman, G. Scalmani, V. Barone, B. Mennucci, G. A. Petersson, G. H. Nakatsuji, M. Caricato, X. Li, H. P. Hratchian, A. F. Izmaylov, J. Bloino, G. Zheng, J. L. Sonnenberg, M. Hada, M. Ehara, K. Toyota, R. Fukuda, J. Hasegawa, M. Ishida, T. Nakajima, Y. Honda, O. Kitao, H. Nakai, T. Vreven, Jr. J. A. Montgomery, J. E. Peralta, F. Ogliaro, M. Bearpark, J. J. Heyd, E. Brothers, K. N. Kudin, V. N. Staroverov, R. Kobayashi, J. Normand, K. Raghavachari, A. Rendell, J. C. Burant, S. S. Iyengar, J. Tomasi, M. Cossi, N. Rega, J. M. Millam, M. Klene, J. E. Knox, J. B. Cross, V. Bakken, C. Adamo, J. Jaramillo, R. Gomperts, R. E. Stratmann, O. Yazyev, A. J. Austin, R. Cammi, C. Pomelli, J. W. Ochterski,

R. L. Martin, K. Morokuma, V. G. Zakrzewski, G. A. Voth, P. Salvador, J. J. Dannenberg, S. Dapprich, A. D. Daniels, Ö. Farkas, J. B. Foresman, J. V. Ortiz, J. Cioslowski, D. J. Fox, Gaussian, Inc., Wallingford CT, **2010**.

(S14) Y. Zhao, N. E. Schultz, D. G. Truhlar, *J. Chem. Theory and Comput*., 2006, **2**, 364-382.

(S15) A. Schäfer, H. Horn, R. Ahlrichs, *J. Chem. Phys*., 1992, **97**, 2571-2577.

(S16) A. Schäfer, C. Huber, R. Ahlrichs, *J. Chem. Phys*., 1994, **100**, 5829-5835.

(S17) A. V. Marenich, C. J. Cramer, D. G. Truhlar, *J. Phys. Chem. B,* 2009, **113**, 6378–6396.

(S18) AIMAll (Version 13.11.04, Standard), Copyright © 1997-2013, T. A. Keith http://aim.tkgristmill.com

(S19) R. F. W. Bader, *Chem. Rev*., 1991, **94**, 893-928

(S20) http://www.chemcraftprog.com.

(S21) A. Pradel, V. Michel-Lledos, M. Ribes, H. Eckert, *Chem. Mater*., 1993, **5**, 377.